

AWARD NUMBER: W81XWH-17-1-0134

TITLE: Interrogating the Mechanism of Long Noncoding RNA ARInc-1 in Regulating AR Signaling

PRINCIPAL INVESTIGATOR: Yajia Zhang

CONTRACTING ORGANIZATION: Regents of the University of Michigan  
Ann Arbor, MI 48109

REPORT DATE: May 2018

TYPE OF REPORT: Annual

PREPARED FOR: U.S. Army Medical Research and Materiel Command  
Fort Detrick, Maryland 21702-5012

DISTRIBUTION STATEMENT: Approved for Public Release;  
Distribution Unlimited

The views, opinions and/or findings contained in this report are those of the author(s) and should not be construed as an official Department of the Army position, policy or decision unless so designated by other documentation.

# REPORT DOCUMENTATION PAGE

Form Approved  
OMB No. 0704-0188

Public reporting burden for this collection of information is estimated to average 1 hour per response, including the time for reviewing instructions, searching existing data sources, gathering and maintaining the data needed, and completing and reviewing this collection of information. Send comments regarding this burden estimate or any other aspect of this collection of information, including suggestions for reducing this burden to Department of Defense, Washington Headquarters Services, Directorate for Information Operations and Reports (0704-0188), 1215 Jefferson Davis Highway, Suite 1204, Arlington, VA 22202-4302. Respondents should be aware that notwithstanding any other provision of law, no person shall be subject to any penalty for failing to comply with a collection of information if it does not display a currently valid OMB control number. **PLEASE DO NOT RETURN YOUR FORM TO THE ABOVE ADDRESS.**

<b>1. REPORT DATE</b> May 2018		<b>2. REPORT TYPE</b> Annual		<b>3. DATES COVERED</b> 1 May 2017- 30 Apr 2018	
<b>4. TITLE AND SUBTITLE</b> Interrogating the Mechanism of Long Noncoding RNA ARlnc-1 in Regulating AR Signaling				<b>5a. CONTRACT NUMBER</b>	
				<b>5b. GRANT NUMBER</b> W81XWH-17-1-0134	
				<b>5c. PROGRAM ELEMENT NUMBER</b>	
<b>6. AUTHOR(S)</b> Yajia Zhang				<b>5d. PROJECT NUMBER</b>	
				<b>5e. TASK NUMBER</b>	
E-Mail: yajiazh@med.umich.edu				<b>5f. WORK UNIT NUMBER</b>	
<b>7. PERFORMING ORGANIZATION NAME(S) AND ADDRESS(ES)</b> Regents of the University of Michigan Ann Arbor, Michigan 48109				<b>8. PERFORMING ORGANIZATION REPORT NUMBER</b>	
<b>9. SPONSORING / MONITORING AGENCY NAME(S) AND ADDRESS(ES)</b> U.S. Army Medical Research and Materiel Command Fort Detrick, Maryland 21702-5012				<b>10. SPONSOR/MONITOR'S ACRONYM(S)</b>	
				<b>11. SPONSOR/MONITOR'S REPORT NUMBER(S)</b>	
<b>12. DISTRIBUTION / AVAILABILITY STATEMENT</b> Approved for Public Release; Distribution Unlimited					
<b>13. SUPPLEMENTARY NOTES</b>					
<b>14. ABSTRACT</b> Prostate cancer is the most commonly diagnosed type of non-skin cancer in American men. It is estimated that ~164,690 new cases will be diagnosed in 2018. Despite the fact that most patients with primary prostate cancer can be cured with androgen deprivation therapy (ADT), in some patients, disease progresses to metastasis state, which is castration-resistant and always lethal. Researchers have been searching for the molecular mechanisms that contribute to the progression of castration resistant prostate cancer (CRPC). One of the mechanisms highlights the continued activation of AR signaling, for example, by AR gene amplification, splicing variants of AR transcript, as well as promiscuous activation of AR. Most of these studies focused on investigating protein-coding genes, meanwhile, the study of lncRNAs associated with AR signaling is lacking. To fulfill this knowledge gap, our lab previously conducted a comprehensive profiling of androgen regulated non-coding transcriptome in cell lines and patient samples. In an effort to identify lncRNAs that are both induced by androgen stimulation, and have elevated expression in primary and metastasis prostate cancer (compared to normal prostate), we discovered a top candidate, ARlnc1. Expression of this lncRNA is highly prostate-lineage specific, driven by AR and FOXA1. Functional investigation of this lncRNA suggested that this lncRNA mediates prostate cancer cell proliferation. Gene expression profiling suggested that ARlnc1 regulates AR signaling. In the current project, we aimed to Interrogate the mechanism of how long non-coding RNA ARlnc1 regulates Androgen Receptor signaling.					
<b>15. SUBJECT TERMS</b> lncRNA, AR signaling, ARlnc1					
<b>16. SECURITY CLASSIFICATION OF:</b> U			<b>17. LIMITATION OF ABSTRACT</b>  UU	<b>18. NUMBER OF PAGES</b>  30	<b>19a. NAME OF RESPONSIBLE PERSON</b> USAMRMC
<b>a. REPORT</b> U	<b>b. ABSTRACT</b> U	<b>c. THIS PAGE</b> U			<b>19b. TELEPHONE NUMBER (include area code)</b>

## Table of Contents

	<u>Page</u>
<b>1. Introduction.....</b>	<b>3</b>
<b>2. Keywords.....</b>	<b>3</b>
<b>3. Accomplishments.....</b>	<b>3</b>
<b>4. Impact.....</b>	<b>15</b>
<b>5. Changes/Problems.....</b>	<b>16</b>
<b>6. Products.....</b>	<b>16</b>
<b>7. Participants &amp; Other Collaborating Organizations.....</b>	<b>17</b>
<b>8. Special Reporting Requirements.....</b>	<b>18</b>
<b>9. Appendices.....</b>	<b>18</b>

## 1. INTRODUCTION:

Prostate cancer is the most commonly diagnosed type of non-skin cancer in American men. It is estimated that ~164,690 new cases will be diagnosed in 2018. Despite the fact that most patients with primary prostate cancer can be cured with androgen deprivation therapy (ADT), in some patients, disease progresses to metastasis state, which is castration-resistant and always lethal. Researchers have been searching for the molecular mechanisms that contribute to the progression of castration resistant prostate cancer (CRPC). One of the mechanisms highlights the continued activation of AR signaling, for example, by AR gene amplification, splicing variants of AR transcript, as well as promiscuous activation of AR. Most of these studies focused on investigating protein-coding genes, meanwhile, the study of lncRNAs associated with AR signaling is lacking. To fulfill this knowledge gap, our lab previously conducted a comprehensive profiling of androgen regulated non-coding transcriptome in cell lines and patient samples. In an effort to identify lncRNAs that are both induced by androgen stimulation, and have elevated expression in primary and metastasis prostate cancer (compared to normal prostate), we discovered a top candidate, ARlnc1. Expression of this lncRNA is highly prostate-lineage specific, driven by AR and FOXA1. Functional investigation of this lncRNA suggested that this lncRNA mediates prostate cancer cell proliferation. Gene expression profiling suggested that ARlnc1 regulates AR signaling. In the current project, we aimed to interrogate the mechanisms of how long non-coding RNA ARlnc1 regulates Androgen Receptor signaling.

## 2. KEYWORDS:

lncRNA, AR, ARlnc1

## 3. ACCOMPLISHMENTS:

### What were the major goals of the project?

To test the hypothesis that ARlnc1 regulates androgen receptor signaling via modulating AR transcript, and that the ARlnc1-AR feed-forward loop provides new therapeutic opportunities for patients with prostate cancer, we proposed the following three aims:

**Specific Aim 1:** To characterize interaction between AR and ARlnc1 *in vitro* and *in vivo*. (Month 1-8.) This Aim is 100% completed.

**Specific Aim 2:** To investigate the molecular mechanism of ARlnc1 in regulating AR transcript stability. (Month 9-15.) This Aim is 60% completed.

**Specific Aim 3:** To evaluate the therapeutic impact of ARlnc1-AR interaction in pre-clinical models. (Month 15-24) This Aim is 0% completed.

## What was accomplished under these goals?

Under each specific aim, the specific objectives, significant results and achievements are described as follows.

**Specific Aim 1:** To characterize interaction between AR and ARlnc1 *in vitro* and *in vivo*. (Month 1-8, Progress: 100% completed)

**Objective 1:** To develop an *in-vitro* RNA-RNA binding assay. (Month 1-3, Progress: 100% completed)

### Methods:

To start to evaluate AR-ARlnc1 interaction *in vitro*, we developed an RNA-RNA binding assay. Briefly, RNA fragments of ARlnc1, ARlnc1-antisense, LacZ, SChLAP1-antisense, and THOR, were synthesized *in vitro* and labeled with Bromouridine (BrU). Equal amounts of BrU-labeled RNA were then incubated with BrU antibody-conjugated Protein G beads. After RNA-antibody-beads conjugation, equal amounts of synthesized AR-5'UTR RNA fragments were added to each tube and allowed to incubate overnight. Following washing, RNA was recovered and the leftover AR 5'UTR amounts were quantified by qPCR analysis.

### Significant results:

Compared to a panel of control RNA fragments (ARlnc1-antisense, LacZ, SChLAP1-antisense, THOR, and beads control), ARlnc1 binds AR 3'UTR with significantly higher affinity (**Figure 1a**). This observation was in accord with an *in silico* assay, where AR 3'UTR was predicted as a potential binding partner of ARlnc1. The RNA-RNA binding assay developed here is the first step in characterizing ARlnc1-AR 3'UTR interaction in cell-free systems.

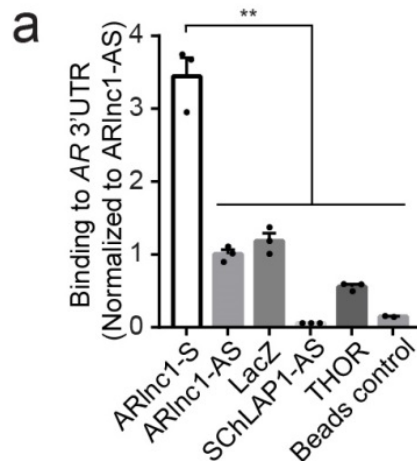


**Figure 1:** (a) Relative binding between AR 3'UTR-1-980 RNA fragment and a panel of BrU-labeled RNAs, measured by *in-vitro* RNA-RNA interaction assay. Data were normalized to ARlnc1-AS control. Mean  $\pm$  s.e.m. are shown,  $n = 3$ .  $**P < 0.001$  (two-tailed Student's t-test).

**Objective 2:** To determine direct interaction sites between ARlnc1 and AR 3'UTR *in vitro*. (Month 1-3, Progress: 100% completed)

**Methods:**

To identify the RNA fragment that mediates the ARlnc1-AR3'UTR interaction, RNA fragments spanning every ~600bp of ARlnc1 were constructed. RNA-RNA binding analysis was performed using methods developed above. Antisense of ARlnc1 was included as control. After pinpointing the fragment on ARlnc1 that mediates the ARlnc1-AR3'UTR interaction, a deleted version of ARlnc1 was constructed and used for RNA-RNA interaction assay as a way of validation.

**Significant results:**

The RNA fragment spanning 700-1300 of ARlnc1 binds to AR3'UTR with the highest affinity (**Figure 2a**), suggesting that this is the critical region mediating the RNA-RNA interaction. In accord with this observation, the deletion construct lacking nucleotides 700-1300 abrogated the binding between ARlnc1 and AR 3'UTR (**Figure 2b**).

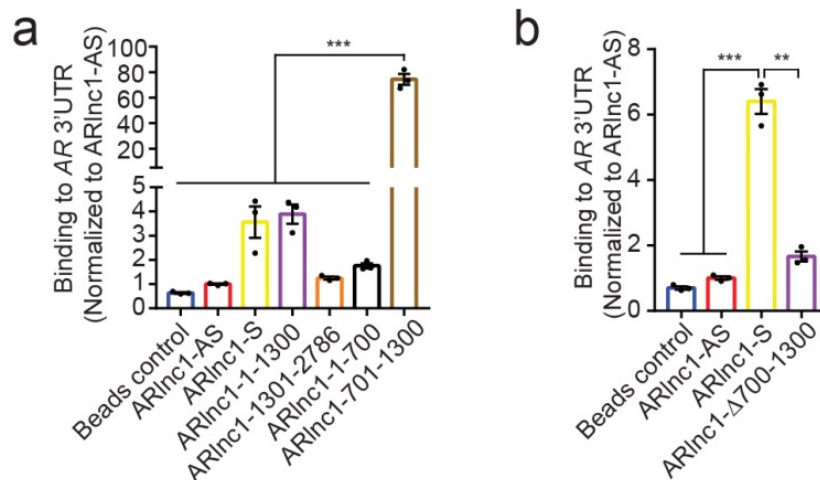


**Figure 2:** (a) Relative binding between AR 3'UTR-1-980 RNA and a panel of BrU labeled RNA fragments spanning ARlnc1. Data were normalized to ARLNC1-AS control. Mean  $\pm$  s.e.m. are shown,  $n = 3$ . \*\*\*Adjusted  $P = 0.0001$  (ANOVA with Dunnett's multiple comparisons test) (b) Relative binding between AR 3'UTR-1-980 RNA and ARlnc1 with 700-1300 deletion, measured by *in-vitro* RNA-RNA interaction assay. Data were normalized to ARlnc1-AS control. Mean  $\pm$  s.e.m. are shown,  $n = 3$ . \*\*\* $P = 0.0001$ , \*\* $P = 0.0003$  (two-tailed Student's t-test).

**Objective 3:** To visualize co-localization of ARlnc1 and AR in cells, using RNA-FISH technology. (Month 6-8, Progress: 100% completed)

**Methods:**

Cellular localization patterns of ARlnc1 and AR transcripts were visualized using single molecular RNA-fluorescence *in situ* hybridization (smFISH) in AR-positive prostate cancer cell line model. Co-localization rate was quantified and compared with control RNA molecules. To verify the interaction sites identified from *in-vitro* experiments, expression constructs coding for different fragments of ARlnc1 were constructed and transfected into U2-OS cells. Co-localization between AR transcript and different ARlnc1 fragments were visualized by smFISH.

**Significant results:**

As shown in Figure 3, co-localization between endogenous ARlnc1 and AR transcripts was observed in MDA-PCa-2b cells (**Figure 3a**). Using a panel of abundant mRNA species as control (EZH2, HMBS, FOXA1, ACTB, and GAPDH), quantified co-localization events between AR and ARlnc1 were significantly higher (**Figure 3b**).

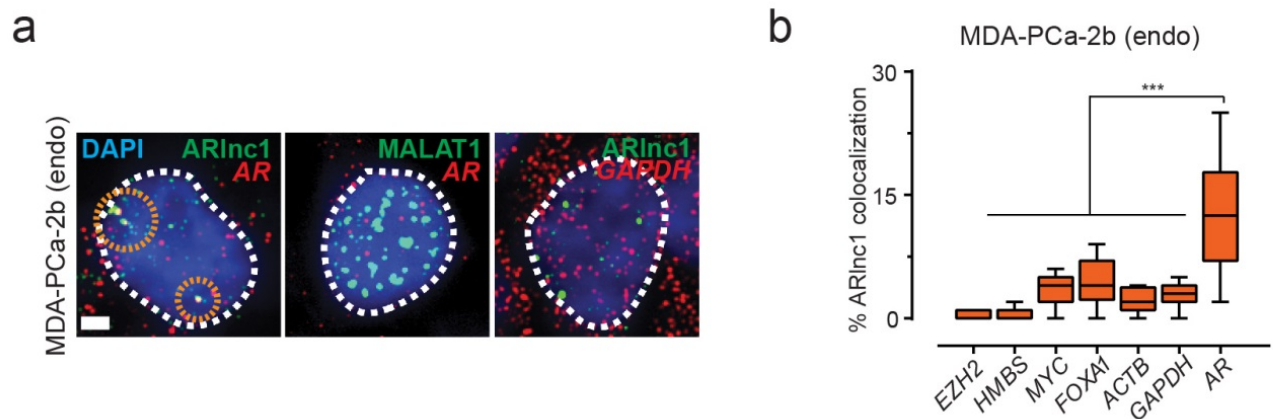


**Figure 3:** smFISH depiction of AR-ARlnc1 colocalization in cells. **(a)** Representative pseudocolored images of MDA-PCa-2b cell nuclei stained for the appropriate endogenous (endo) transcripts and DAPI. Scale bar, 5  $\mu$ m. Orange circles represent regions of colocalization. **(b)** Quantification of the percentage of ARlnc1 molecules co-localizing with a panel of mRNAs. Center lines and whiskers depict the median and range, respectively, and box extends from 25th to 75th percentiles ( $n = 50$  cells for each sample aggregated from 3 independent experiments). \*\*\* $P < 0.0001$  by two-tailed Student's t-test.

To further validate the RNA-RNA interaction sites identified *in vitro*, U2-OS cells were co-transfected with AR-full length expression construct and constructs encoding various ARlnc1-fragments. In this exogenous system, we found a higher co-localization rate between AR transcript and ARlnc1 RNA fragments containing nucleotide 700-1300 (compared to RNA fragments lacking 700-1300 sites)(**Figure 4**).

Therefore, the co-localization between ARlnc1 and AR transcripts was verified in both endogenous system and exogenous system *in situ*. The 700-1300 sites on ARlnc1 are critical in mediating this co-localization.

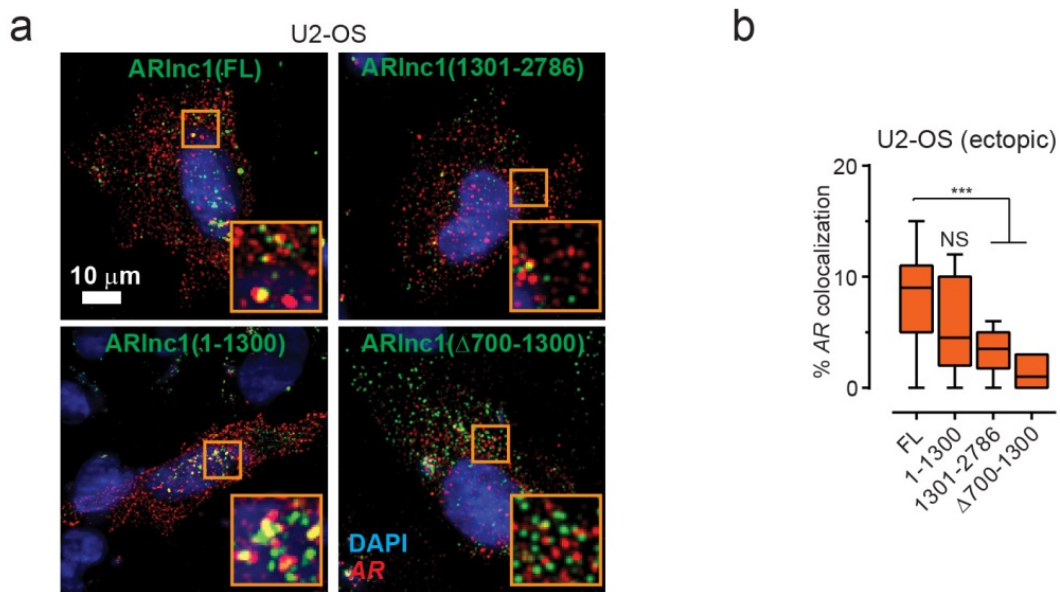


**Figure 4:** (a-b) smFISH showing that 700-1300nt in ARInc1 is critical for co-localization in situ. (a) Representative pseudo-colored images of U2-OS cells stained for DAPI (nucleus), ARInc1 and AR transcripts (smFISH). Scale bar, 10 μm. Inset, 10x10 μm<sup>2</sup> zoomed-in view of orange box in the image. (b) Quantification of the percent of AR molecules colocalizing with various ARInc1 fragments. Center line and whiskers depict the median and range respectively and box extends from 25th to 75th percentiles (n = 50 cells for each sample aggregated from 3 independent experiments). \*\*\* $P < 0.0001$  by two-tailed Student's t-test. NS: not significant.

**Objective 4:** To detect functional ARInc1-AR mRNA interaction in cells, using RNA antisense purification (RAP) technology followed by qPCR. (Month 4-6, Progress: 100% completed)

**Methods:**

In order to detect the functional ARInc1-AR interaction in cells, we initially proposed to perform RNA antisense purification (RAP) followed by qPCR analysis. However, after several rounds of assay optimization for the RAP-qPCR technology, we found that RAP-based RNA-binding partner detection method had low efficacy. Therefore, we utilized a slightly different approach: we applied antisense oligonucleotides to interfere with the identified RNA-RNA binding sites in cells, and tried to detect changes of co-localization

between ARlnc1 and AR RNA molecules. We further evaluated the AR signaling gene expression to validate that the RNA-RNA interaction is functional in cells.

### Significant results:

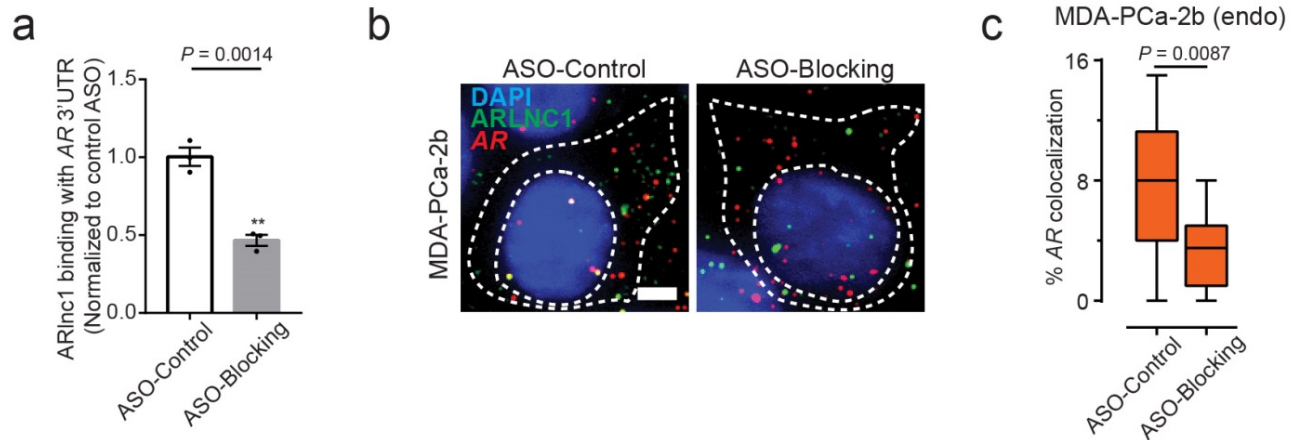


**Figure 5:** (a) *In vitro* RNA-RNA interaction assays between ARlnc1 and AR 3'UTR, with the addition of blocking ASO pool or control ASO. Data were normalized to control ASO. Mean  $\pm$  s.e.m. are shown,  $n = 3$ .  $P = 0.0014$  (unpaired Student's *t*-test). (b) Representative image of smFISH showing that ASOs targeting 700-1300nt on ARlnc1 transcript (ASO-Blocking) inhibit ARlnc1 colocalization with AR in cells. (c) Quantification of the percent of AR transcripts colocalizing with ARlnc1 after various treatments in MDA-PCa-2b cells. Center lines and whiskers depict the median and range and box extends from 25th to 75th percentiles ( $n = 50$  cells for each sample aggregated from 3 independent experiments, unpaired *t* test.)

We first validated the efficacy of blocking ASOs *in vitro* using RNA-RNA binding assay (Figure 5a). Transfecting these blocking ASOs into cells resulted in a decreased colocalization rate between ARlnc1 and AR transcripts, visualized by smFISH (Figure 5b-c). Functionally, disrupting this interaction led to a modest decrease of AR transcript level, thus attenuating AR signaling (Figure 6a). Together, these results suggested the existence of functional ARlnc1-AR interaction in cells. This interaction sustains AR-signaling in ARlnc1-positive cellular contexts.

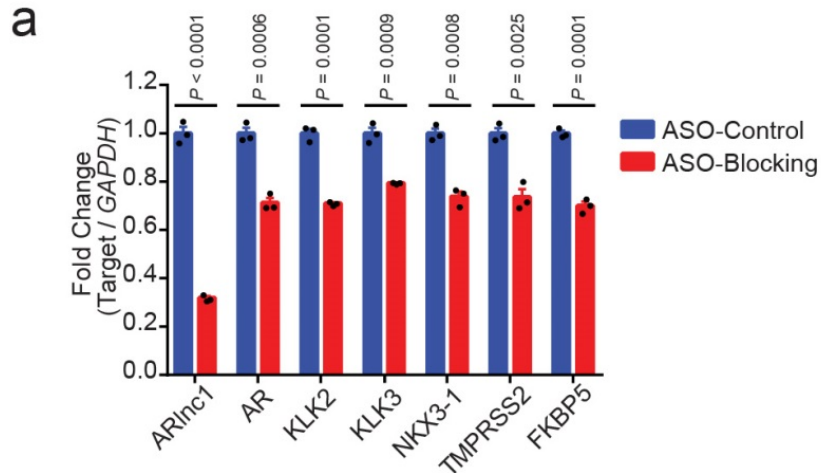


**Figure 6:** (a) qPCR analysis of ARLNC1, AR, and AR signaling genes (KLK2, KLK3, NKX3.1, TMPRSS2, FKBP5) in MDA-PCa-2b cells transfected with control or blocking ASOs targeting the interaction sites between ARLNC1 and AR 3'UTR. Mean  $\pm$  s.e.m. are shown,  $n = 3$ . Significance was determined by two-tailed Student's t-test.

**Objective 5:** Visualize co-localization of ARlnc1 and AR in patient samples. (Month 6-8, Progress: 100% completed)

**Methods:**

To investigate the clinical-relevance of the identified ARlnc1-AR co-localization, we performed smFISH in prostate cancer tissue samples with ARlnc1 expression.

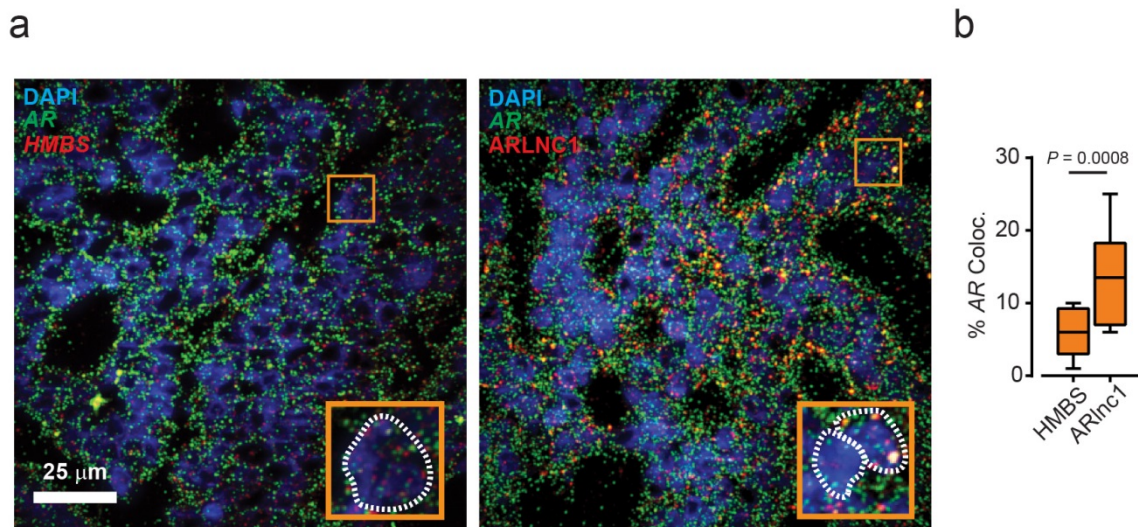


**Figure 7:** Representative pseudo-colored images of ARInc1 positive prostate cancer tissues (**a**) stained with DAPI (nucleus) and AR, HMBS or ARInc1 transcripts (smFISH). Scale bar, 25  $\mu\text{m}$ . Inset, 5.5x5.5  $\mu\text{m}^2$  zoomed-in view of box within large panel. Quantification of the percentage of AR molecules (**b**) colocalizing with HMBS or ARInc1 is also depicted in box plot. Center line and whiskers depict the median and range respectively and box extends from 25th to 75th percentiles ( $n = 15$  field-of-views aggregated for each sample aggregated from 3 independent tissues).  $**P < 0.001$  by two-tailed Student's t-test.

### **Significant results:**

As shown in Figure 7, compared to an abundant control RNA, HMBS, ARInc1 co-localizes with AR at a significantly higher rate. This observation echoes our previous findings in cell line models, further suggesting the functional importance of ARInc1-AR co-localization in prostate cancer patients.

**Specific Aim 2:** To investigate the molecular mechanism of ARInc1 in regulating AR transcript stability. (Month 9-15. Progress: This Aim is 60% completed.)

**Objective 1:** To study whether ARInc1 affects AR 3'UTR activity, using luciferase assay. (Month 9-11. Progress: This Objective is 100% completed)

### **Methods:**

Dual-luciferase assay was performed in ARInc1-positive cells using an AR 3'UTR reporter system containing 3.2kb of AR 3'UTR in front of a luciferase reporter. An empty vector without AR 3'UTR was used as control.

### **Significant results:**

As a positive control, transfection of AR siRNA targeting the 3'UTR region significantly reduced the luciferase activity in MDA-PCa-2b cells. Meanwhile, attenuated AR 3'UTR luciferase activity was observed upon loss of ARInc1, suggesting that the activity of AR 3'UTR is affected by ARInc1 (**Figure 8**). Over-expression of ARInc1 had modest effect of AR 3'UTR activity (**Figure 8**).

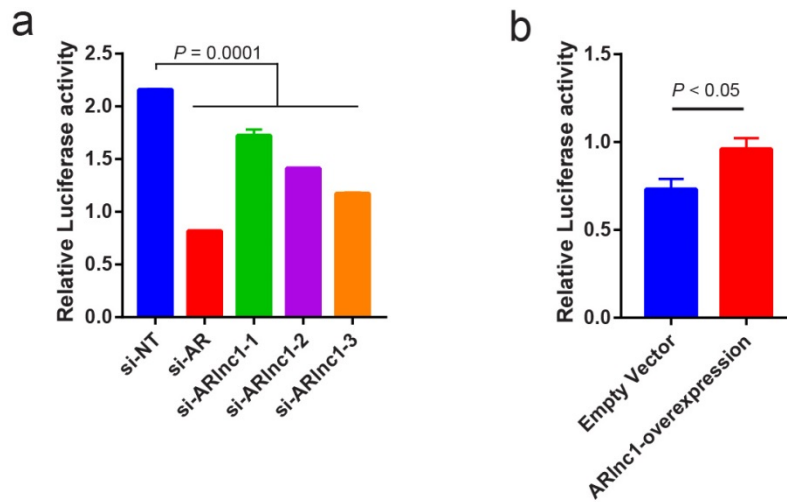


**Figure 8:** Relative luciferase activity of AR 3'UTR under ARInc1 loss (a) or ARInc1-overexpression (b) condition.  $n = 5$ ,  $P$  values calculated from ANOVA (a) or unpaired t test (b).

**Objective 2:** To validate ELAV1 as an ARInc1-interacting protein and determine whether ARInc1 affects binding between ELAV1 and AR 3'UTR. (Month 11-13. Progress: This Objective is 100% completed.)

#### Methods:

Reciprocal interaction between ELAV1 and ARInc1 was tested *in vitro* and in cells by RNA immune-precipitation (RIP) and western blotting analysis.

#### Significant results:

ELAV1 protein was previously reported as an AR 3'UTR-binding protein that mediates AR transcript stability. To start to evaluate the involvement of ELAV1 in ARInc1-mediated AR signaling regulation, we first assessed the binding between ELAV1 protein and ARInc1 *in vitro*. Using ARInc1-AS as control, we detected binding of HuR to ARInc1-S using western-blotting analysis (**Figure 9a**). This interaction followed a dose-dependent pattern (**Figure 9b**). We further performed RNA-immunoprecipitation using HuR antibody in MDA-PCa-2b cells. Relative enrichment of ARInc1 RNA suggested that HuR-ARInc1 interaction exists in cells (**Figure 9c**). To investigate whether ARInc1 affects HuR-binding to AR transcript, RIP-qPCR analysis was conducted under ARInc1-loss condition or control condition (**Figure 9d**). Without ARInc1, the AR-HuR binding decreased significantly, while the control Actin-HuR binding intensity remained the

same. These results suggested that ARlnc1 is involved in mediating binding between HuR and AR transcript.

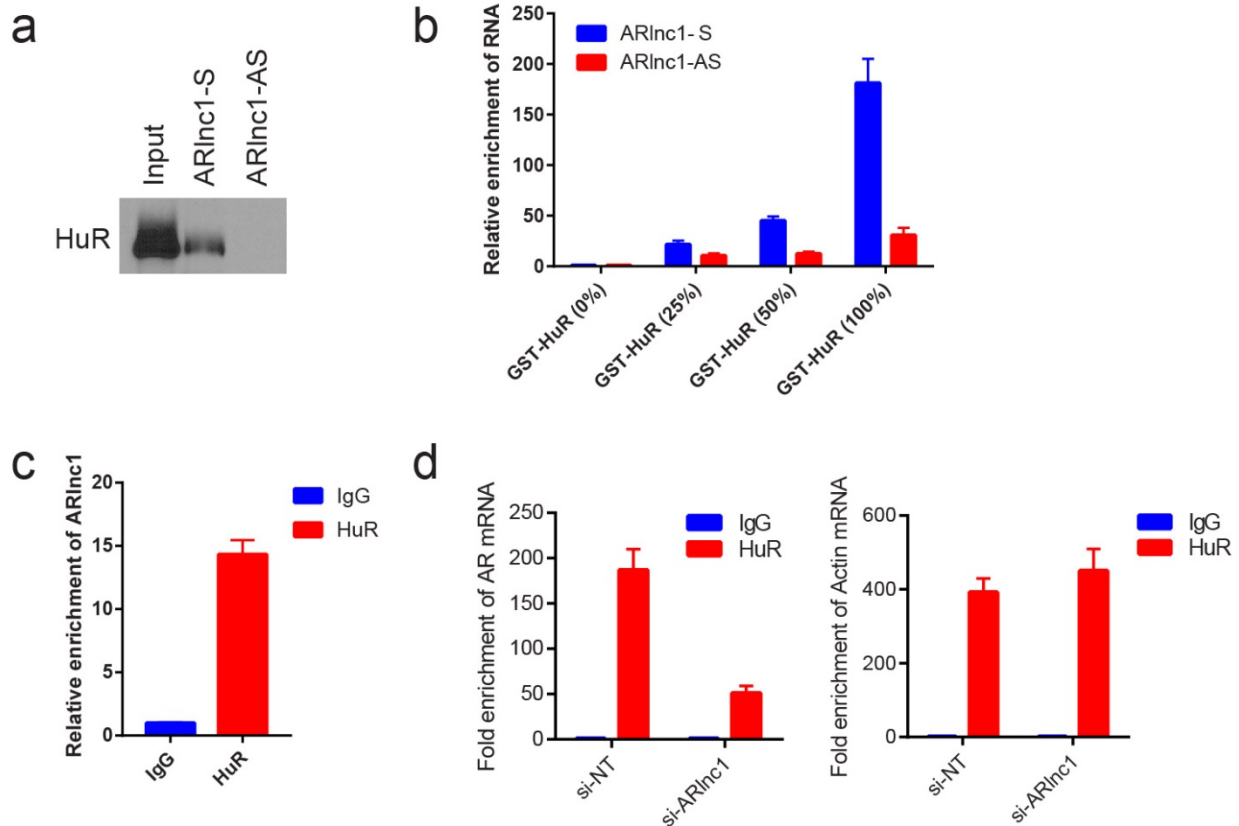


**Figure 9:** (a) Relative binding of HuR protein to ARlnc1-S or ARlnc1-AS RNA, evaluated by western blotting. (b) Dose-dependent binding of ARlnc1 to GST-HuR, following GST-pull down. Relative RNA enrichment was assessed by qPCR. (c) RIP-qPCR analysis indicating the binding between HuR protein and ARlnc1 in MDA-PCa-2b cells. (d) Relative binding between HuR protein and AR mRNA or Actin mRNA, under control or ARlnc1-knockdown condition. Binding was quantified by RIP-qPCR analysis in MDA-PCa-2b cells.

**Objective 3:** Assess whether ARlnc1 regulates AR 3'UTR activity via ELAV1 (Month 13-15. Progress: This Objective is 0% completed.)

**Specific Aim 3:** To evaluate the therapeutic impact of ARlnc1-AR interaction in pre-clinical models. (Month 15-24) This Aim is 0% completed. The planned experiments will be completed during the next research cycle.

## **What opportunities for training and professional development has the project provided?**

The project has provided several opportunities for training and professional development, which includes:

(1) **One-on-one meeting with mentor:** Research progress was discussed with my mentor during bi-weekly individual meetings. Dr. Chinnaiyan provides guidance and advice to the project and closely oversees the work. Research progress reports were submitted monthly.

(2) **Weekly department seminars:** Routinely attended the Pathology Department weekly seminar and RNA innovation seminar at University of Michigan.

(3) **Group meeting and lab meeting:** Results generated from the project was presented and discussed during lncRNA group meetings and lab meetings.

(4) **Presentations at conference:**

Platform talk: *Molecular and Cellular Department Annual Retreat* Nov. 2017, University of Michigan-Ann Arbor, Michigan.

Poster presentation: *Prostate Specialized Programs of Research Excellence (SPORE) Annual Meeting* Feb. 2018, Ft. Lauderdale, Florida.

Poster presentation: *AACR Annual meeting* Apr. 2018, Chicago, Illinois.

## **How were the results disseminated to communities of interest?**

Results from this project were presented at conferences, including the *AACR Annual meeting* (Apr. 2018), and the *Prostate Specialized Programs of Research Excellence (SPORE) Annual Meeting* (Feb. 2018). A manuscript containing the results generated from this project will be published during the next reporting cycle.

## **What do you plan to do during the next reporting period to accomplish the goals?**

In the next research cycle, we anticipate to complete all of the remaining parts in specific aims 2 and 3 as planned. Specifically, we plan to achieve these objectives:

Specific Aim 2: To investigate the molecular mechanism of ARlnc1 in regulating AR transcript stability. (Month 9-15. Progress: This Aim is 60% completed.)

Objective: Assess whether ARInc1 regulates AR 3'UTR activity via ELAV1 (Month 13-15. Progress: This Objective is 0% completed.)

Specific Aim 3: To evaluate the therapeutic impact of ARInc1-AR interaction in pre-clinical models. (Month 15-24) This Aim is 0% completed.

Objective 1: To develop lentiviral construct containing inducible shRNA targeting ARInc1 and generate stable cell lines. Examine impact of ARInc1-depletion on tumor growth.

Objective 2: To evaluate the phenotypic effect of blocking ASOs against ARInc1-AR interacting sites *in vitro*.

Objective 3: To evaluate the therapeutic potential of ARInc1 *in vivo*, using cell line derived xenografts.

By the end of the next reporting period, we anticipate to have published a manuscript describing results on ARInc1.

#### **4. IMPACT:**

##### **What was the impact on the development of the principal discipline(s) of the project?**

Once completed, the research project "Interrogating the mechanism of long non-coding RNA ARInc-1 in regulating AR signaling" will have significant impact on understanding lncRNA functional mechanism and their roles in regulating androgen receptor in prostate cancer context. We proposed to investigate the involvement of lncRNA-mRNA, lncRNA-protein interactions in regulating transcript stability. We also proposed to test whether these mechanisms provide a novel node for targeting prostate cancer therapeutically.

During the reported research cycle, we have established the RNA-RNA interaction between ARInc1 and AR transcript in both cell-free system and cell line models. Co-localization of these RNAs was observed in cells and in prostate cancer tissues. Loss of ARInc1 impairs AR transcript stability, and this process may be mediated by another RNA-binding protein, ELAV1.

We anticipate that by the end of next research cycle, we will be able to delineate the mechanism of how ARInc1 regulates AR signaling, and to establish lncRNAs as a novel therapeutic node in prostate cancer.

**What was the impact on other disciplines?**

Nothing to Report

**What was the impact on technology transfer?**

Nothing to Report

**What was the impact on society beyond science and technology?**

Nothing to Report

**5. CHANGES/PROBLEMS:**

**Changes in approach and reasons for change**

Nothing to Report

**Actual or anticipated problems or delays and actions or plans to resolve them**

Nothing to Report

**Changes that had a significant impact on expenditures**

Nothing to Report

**Significant changes in use or care of human subjects, vertebrate animals, biohazards, and/or select agents**

Nothing to Report

**Significant changes in use or care of human subjects**

Nothing to Report

**Significant changes in use or care of vertebrate animals**

Nothing to Report

**Significant changes in use of biohazards and/or select agents**

Nothing to Report

**6. PRODUCTS:**

**Journal Publications:** Nothing to Report

**Other publications, conference papers, and presentations:**

Poster presentation and Abstract: **Yajia Zhang**, Sethuramasundaram Pitchiaya, Marcin Cieřlik, Yashar S. Niknafs, Jean C-Y. Tien, Yasuyuki Hosono, Matthew K. Iyer, Lisha Wang, Yuanyuan Qiao, Xuhong Cao, Mats Ljungman, Hui Jiang, Rohit Mehra, Shuling Guo, John T. Wei, Felix Y. Feng, Rohit Malik, Arul M. Chinnaiyan. **The Androgen Receptor-Regulated LncRNA Landscape Reveals a Role for ARlnc1 in Prostate Cancer Progression.** [abstract]. In: *Proceedings of the 109th Annual Meeting of the American Association for Cancer Research*; 2018 Apr 14-18; Chicago, IL, AACR.

Poster: **Yajia Zhang**, Rohit Malik, Marcin Cieslik, Sethuramasundaram Pitchiaya, Jean Ching-Yi Tien, Yashar Niknafs, Yasuyuki Hosono, Sahr Yazdani, Xuhong Cao, Dan Robinson and Arul Chinnaiyan. **Investigating the role of androgen receptor regulated long non-coding RNA ARlnc1 in prostate cancer.** *Keystone Symposia Conference- Noncoding RNAs: From Disease to Targeted Therapeutics*, 2017

Other publication: Alexander R. Gawronski, Michael Uhl, **Yajia Zhang**, Yen-Yi Lin, Yashar S. Niknafs, Varune R. Ramnarine, Rohit Malik, Felix Feng, Arul M. Chinnaiyan, Colin C. Collins, S. Cenk Sahinalp, Rolf Backofen. **MechRNA: prediction of lncRNA mechanisms from RNA–RNA and RNA–protein interactions.** *Bioinformatics*, 03 Apr 2018.

**Website(s) or other Internet site(s):** Nothing to Report

**Technologies or techniques:** Nothing to Report

**Inventions, patent applications, and/or licenses:** Nothing to Report

**Other Products:** Nothing to Report

## 7. PARTICIPANTS & OTHER COLLABORATING ORGANIZATIONS:

**What individuals have worked on the project?**

Name:	<i>Yajia Zhang</i>
Project Role:	<i>Graduate Student</i>
Researcher Identifier (e.g. ORCID ID):	N/A
Nearest person month worked:	6.0
Contribution to Project:	<i>Ms. Zhang has performed work in the area of prostate cancer biology, especially discovering functioning mechanism of long non-coding RNAs in cancer context.</i>
Funding Support:	N/A

**Has there been a change in the active other support of the PD/PI(s) or senior/key personnel since the last reporting period?**

Nothing to Report

**What other organizations were involved as partners?**

Nothing to Report

## **8. SPECIAL REPORTING REQUIREMENTS**

Not Applicable

## **9. APPENDICES**

1. CV\_Yajia Zhang
2. Other publication: Alexander R. Gawronski, Michael Uhl, **Yajia Zhang**, Yen-Yi Lin, Yashar S. Niknafs, Varune R. Ramnarine, Rohit Malik, Felix Feng, Arul M. Chinnaiyan, Colin C. Collins, S. Cenk Sahinalp, Rolf Backofen. **MechRNA: prediction of lncRNA mechanisms from RNA–RNA and RNA–protein interactions.** *Bioinformatics*, 03 Apr 2018.

## Yajia Zhang

Tel: 734-730-4109 • E-mail: [yajiazh@umich.edu](mailto:yajiazh@umich.edu)

### Education

- Sept.2014- present     PhD candidate, Program of Molecular and Cellular Pathology,  
University of Michigan Medical School, Ann Arbor, MI  
Cumulative GPA: 3.904  
Thesis Advisor: Arul Chinnaiyan, MD, PhD
- Sept.2013- Sept.2014     Graduate student, Program in Biomedical Sciences, University of Michigan  
Medical School, Ann Arbor, MI  
Rotation Advisors: Scott Tomlins, MD, PhD; David Lombard, MD, PhD
- Sept. 2009- Jun.2013     Bachelor of Science, College of Life Sciences, Nankai University, Tianjin, China  
Major: Biological Science  
Cumulative GPA: 91.1/ 100 (3.86/ 4.0)  
GRE: 330/340 (Verbal: 161, Quantitative: 169)

### Published Works

Alexander R. Gawronski, Michael Uhl, **Yajia Zhang**, Yen-Yi Lin, Yashar S. Niknafs, Varune R. Ramnarine, Rohit Malik, Felix Feng, Arul M. Chinnaiyan, Colin C. Collins, S. Cenk Sahinalp, Rolf Backofen. **MechRNA: prediction of lncRNA mechanisms from RNA–RNA and RNA–protein interactions.** *Bioinformatics*, 03 Apr 2018, <https://doi.org/10.1093/bioinformatics/bty208>

Andrew S. McDaniel, Daniel H. Hovelson, Andi K. Cani, Chia-Jen Liu, Yali Zhai, **Yajia Zhang**, Alon Z. Weizer, Rohit Mehra, Felix Y. Feng, Ajjai S. Alva, Todd M. Morgan, Jeffrey S. Montgomery, Javed Siddiqui, Seth Sadis, Santhoshi Bandla, Paul D. Williams, Kathleen R. Cho, Daniel R. Rhodes, Scott A. Tomlins. **Genomic profiling of penile squamous cell carcinoma reveals new opportunities for targeted therapy.** *Cancer Research*, 15 Dec 2015, 75(24): 5219-27

### Poster and Conference Presentations

Poster: **Yajia Zhang**, Sethuramasundaram Pitchiaya, Marcin Cieřlik, Yashar S. Niknafs, Jean C-Y. Tien, Yasuyuki Hosono, Matthew K. Iyer, Lisha Wang, Yuanyuan Qiao, Xuhong Cao, Mats Ljungman, Hui Jiang, Rohit Mehra, Shuling Guo, John T. Wei, Felix Y. Feng, Rohit Malik, Arul M. Chinnaiyan. **The Androgen Receptor-Regulated lncRNA Landscape Reveals a Role for ARlnc1 in Prostate Cancer Progression.** [abstract]. In: *Proceedings of the 109th Annual Meeting of the American Association for Cancer Research*; 2018 Apr 14-18; Chicago, IL, AACR.

Poster: **Yajia Zhang**, Rohit Malik, Marcin Cieslik, Sethuramasundaram Pitchiaya, Jean Ching-Yi Tien, Yashar Niknafs, Yasuyuki Hosono, Sahr Yazdani, Xuhong Cao, Dan Robinson and Arul Chinnaiyan. **Investigating the role of androgen receptor regulated long non-coding RNA ARlnc1 in prostate cancer.** *Keystone Symposia Conference- Noncoding RNAs: From Disease to Targeted Therapeutics*, 2017

Poster: Rohit Malik, **Yajia Zhang**, Marcin Cieslik, Yashar S. Niknafs, Sethuramasundaram Pitchiaya, Yasuyuki Hosono, Shruthi Subramaniam, Sahr Yazdani, Xuhong Cao, Dan Robinson, Arul Chinnaiyan. **Integrative analysis of androgen receptor regulated long non-coding RNA in prostate cancer.** [abstract]. In: *Proceedings of the 107th Annual Meeting of the American Association for Cancer Research*; 2016 Apr 16-20; New Orleans, Louisiana, AACR; *Cancer Res* 2016;76 (14 Suppl.):Abstract 983.

Poster: **Yajia Zhang**, Rohit Malik, Jean Tien, Christine Brennan, Beth Lawlor, Arul Chinnaiyan. **Targeting EWSR1 as a therapeutic method to treat Ewing Sarcoma** *Molecular and Cellular Pathology Annual Symposium*, University of Michigan, 2015

Platform talk and poster presentation: **Yajia Zhang**, Anmol Amin, Venkata Yadati, Andi Cani, Chia-Jen Liu, Michael J. Quist, Andrew McDaniel, Catherine S. Grasso, Scott A. Tomlins **Targeted next generation sequencing of epithelioid angiomyolipoma identifies germline BRCA2 variants in young patients** *5<sup>th</sup> Annual Anatomic, Molecular, Hematopathology Research Day*, University of Michigan, 2014

## **Awards & Honors**

- 2018 Rackham Conference Travel Grant
- 2017 Department of Defense- FY16 Prostate Cancer Research Program- Early Investigator Research Award (Predoctoral, #PC160970)
- 2017 Rackham International Travel Grant
- 2014 Research Day Abstract Award, 5<sup>th</sup> Annual Anatomic, Molecular, Hematopathology Research Day at University of Michigan (Project: Targeted Next Generation Sequencing of epithelioid angiomyolipoma identifies germline BRCA2 variants in young patients)
- 2012 First Prize of Excellent Undergraduate Scholarship of Nankai University
- 2012 Creative Research Award for the undergraduates of Nankai University (Third Prize)
- 2010 *Kechang Wang* Scholarship
- 2009 Excellent Freshman Scholarship of Nankai University

RNA Biology

## MechRNA: prediction of lncRNA mechanisms from RNA-RNA and RNA-protein interactions

Alexander R. Gawronski<sup>1,\*</sup>, Michael Uhl<sup>3</sup>, Yajia Zhang<sup>6,7</sup>, Yen-Yi Lin<sup>1,2</sup>,  
Yashar S. Niknafs<sup>5</sup>, Varune R. Ramnarine<sup>2</sup>, Rohit Malik<sup>5,11</sup>, Felix Feng<sup>5,9,10</sup>,  
Arul M. Chinnaiyan<sup>5,6,7,8</sup>, Colin C. Collins<sup>2</sup>, S. Cenk Sahinalp<sup>2,4,\*</sup>, Rolf  
Backofen<sup>3,\*</sup>

<sup>1</sup> Computing Science, Simon Fraser University, Burnaby, Canada

<sup>2</sup> Vancouver Prostate Centre, Vancouver, BC, Canada

<sup>3</sup> Institut für Informatik, University of Freiburg, Freiburg im Breisgau, Germany

<sup>4</sup> Department of Computer Science, Indiana University, Bloomington, USA

<sup>5</sup> Michigan Center for Translational Pathology, University of Michigan, Ann Arbor, Michigan 48109, USA

<sup>6</sup> Department of Pathology, University of Michigan, Ann Arbor, Michigan 48109, USA

<sup>7</sup> Department of Computational Medicine and Bioinformatics, Ann Arbor, Michigan 48109, USA

<sup>8</sup> Howard Hughes Medical Institute, University of Michigan, Ann Arbor, Michigan 48109, USA

<sup>9</sup> Department of Radiation Oncology, University of Michigan, Ann Arbor, Michigan 48109, USA

<sup>10</sup> Present address: Departments of Radiation Oncology, Urology, and Medicine, UCSF, San Francisco, California 94115, USA

<sup>11</sup> Present address: Bristol-Myers Squibb Co., Princeton, New Jersey 08543, USA

\*To whom correspondence should be addressed.

Associate Editor: XXXXXXXX

Received on XXXXX; revised on XXXXX; accepted on XXXXX

### Abstract

**Motivation:** Long non-coding RNAs (lncRNAs) are defined as transcripts longer than 200 nucleotides that do not get translated into proteins. Often these transcripts are processed (spliced, capped, polyadenylated) and some are known to have important biological functions. However, most lncRNAs have unknown or poorly understood functions. Nevertheless, because of their potential role in cancer, lncRNAs are receiving a lot of attention, and the need for computational tools to predict their possible mechanisms of action is more than ever. Fundamentally, most of the known lncRNA mechanisms involve RNA-RNA and/or RNA-protein interactions. Through accurate predictions of each kind of interaction and integration of these predictions, it is possible to elucidate potential mechanisms for a given lncRNA.

**Approach:** Here we introduce MechRNA, a pipeline for corroborating RNA-RNA interaction prediction and protein binding prediction for identifying possible lncRNA mechanisms involving specific targets or on a transcriptome-wide scale. The first stage uses a version of IntaRNA2 with added functionality for efficient prediction of RNA-RNA interactions with very long input sequences, allowing for large-scale analysis of lncRNA interactions with little or no loss of optimality. The second stage integrates protein binding information pre-computed by GraphProt, for both the lncRNA and the target. The final stage involves inferring the most likely mechanism for each lncRNA/target pair. This is achieved by generating candidate mechanisms from the predicted interactions, the relative locations of these interactions and correlation data, followed by selection of the most likely mechanistic explanation using a combined p-value.

**Results:** We applied MechRNA on a number of recently identified cancer-related lncRNAs (PCAT1, PCAT29, ARLnc1) and also on two well-studied lncRNAs (PCA3 and 7SL). This led to the identification of hundreds of high confidence potential targets for each lncRNA and corresponding mechanisms. These predictions include the known competitive mechanism of 7SL with HuR for binding on the tumor suppressor TP53, as well as mechanisms expanding what is known about PCAT1 and ARLnc1 and their targets BRCA2 and AR, respectively. For PCAT1-BRCA2, the mechanism involves competitive binding with HuR, which we confirmed using HuR immunoprecipitation assays.

**Availability:** MechRNA is available for download at <https://bitbucket.org/compbio/mechrna>

**Contact:** backofen@informatik.uni-freiburg.de, cenksahi@indiana.edu

**Supplementary information:** Supplementary data are available at *Bioinformatics* online.

## 1 Introduction

With the advance of large-scale transcriptome analysis it has become evident that the majority of the human genome is transcribed into RNA (Djebali *et al.*, 2012). Out of all currently annotated genes, only a minority is known to code for proteins, while most are believed to be non-coding RNAs (ncRNAs). Beside several small ncRNAs, including small nucleolar RNAs (snoRNAs) and microRNAs (miRNAs), manifold analyses showed that especially long non-coding RNAs (lncRNAs), a designation given to any ncRNA longer than 200 nucleotides, play an important role in cell regulation (Marchese *et al.*, 2017). The major classes of lncRNAs include natural antisense transcripts (NATs), promoter-associated ncRNAs (pncRNAs), pseudogenes and long intergenic non-coding RNAs (lincRNAs). They have a variety of known functions influencing transcription, splicing, mRNA stability and translation (Kung *et al.*, 2013).

For some lncRNAs the specific mechanism of action is known, however often only isolated examples exist. For many others the precise mechanism still needs to be determined. At the most fundamental level, every lncRNA mechanism involves RNA-RNA interaction and/or RNA-protein interaction (and via proteins, DNA interactions). So in order to model lncRNA mechanisms computationally, algorithms for predicting these kinds of interactions are essential. There are a number of tools to predict RNA-RNA interactions. These follow four general approaches, in order of complexity: hybridization-only (RNAHybrid (Rehmsmeier *et al.*, 2004), RNADuplex (Lorenz *et al.*, 2011)), sequence concatenation (PairFold (Andronescu *et al.*, 2005), RNACofold (Bernhart *et al.*, 2006)), accessibility-based (RNAup (Muckstein *et al.*, 2006), IntaRNA2 (Mann *et al.*, 2017)) and full joint structure prediction - leading to the first joint free energy model for interacting RNA strands (Alkan *et al.*, 2006) and follow up work (piRNA (Chitsaz *et al.*, 2009), inRNAs (Salari *et al.*, 2010), RIP (Huang *et al.*, 2009)). Hybridization-only methods, where only intermolecular base-pairing is considered, and sequence concatenation methods, where standard algorithms for secondary structure prediction are applied to the concatenation of the input RNA, are very fast but produce unrealistic interactions. Accessibility-based tools compute the partition function of each input sequence and determine the energy required for any given region to be unpaired. These energies are then used as penalties when predicting hybridizations. At the expense of a little higher complexity, the modelled interactions are much more realistic. Accessibility-based tools are efficient enough to have been successfully applied to prokaryotic sRNA and eukaryotic miRNA target prediction on a transcriptome-wide scale. However, due to the complexity of these algorithms, the problem of predicting lncRNA interactions on a transcriptome-wide scale quickly becomes intractable for any method more complex than hybridization-only predictions.

It is possible to use RNA-RNA interaction prediction software for transcriptome-wide, lncRNA-RNA interaction prediction, through the use of existing tools such as IntaRNA (on a supercomputer (Terai *et al.*, 2016)) or by new pipelines such as RISearch2 (Alkan *et al.*, 2017). All these approaches need to apply the following steps (not necessarily in order): (1) determine accessible regions on every target sequence (e.g. using Raccess (Kiryu *et al.*, 2011) and remove repeat regions); (2) determine "seeds" with perfect complementary and extend each seed with flanking sequences of fixed length; and (3) predict (and refine) the interaction between the lncRNA and each of these sequences (e.g. using IntaRNA or RactIP (Kato *et al.*, 2010)). Unfortunately the targets of non-coding RNAs identified through the above approach are typically not very specific. For short non-coding RNAs such as sRNAs and miRNAs, it is possible to improve specificity via sequence conservation (Wright *et al.*, 2013,

2014) across species. However this does not extend to lncRNAs, which are typically poorly conserved (Iyer *et al.*, 2015). As we will discuss below, one way to improve specificity may be to incorporate RNA-protein interactions with RNA-RNA interactions with RNA-protein interactions.

RNA-protein interactions can be determined experimentally using CLIP-Seq, which is currently the standard protocol for the transcriptome-wide identification of RNA-binding protein (RBP) binding sites. Several protocol variants exist, most notably PAR-CLIP (photoactivatable-ribonucleoside-enhanced CLIP) (Hafner *et al.*, 2010) and iCLIP (individual-nucleotide CLIP) (Konig *et al.*, 2010). Lately, eCLIP (enhanced CLIP) (Van Nostrand *et al.*, 2016) and irCLIP (infrared-CLIP) (Zarnegar *et al.*, 2016) have been introduced to further improve protocol efficiency with varying approaches, as discussed in (Uhl *et al.*, 2017).

A drawback of CLIP-Seq protocols to identify RBP binding sites is that they naturally rely on the expression of the target transcripts, which is often cell- or tissue-specific, especially in the case of lncRNAs (Brunner *et al.*, 2012; Liu *et al.*, 2016). Computational prediction of missing binding sites is therefore in high demand. While initial prediction methods such as MEME (Bailey and Elkan, 1994) have relied solely on sequence information, more recent tools like MEMERIS (Hiller *et al.*, 2006), RNAcontext (Kazan *et al.*, 2010) and GraphProt (Maticzka *et al.*, 2014) also incorporate structural information to further improve their predictions.

To our knowledge, no tool exists that integrates both RNA-RNA and RNA-protein interactions. This is crucial for lncRNA interaction prediction since their long length increases the probability of protein binding. The type of RBP, whether it binds to the lncRNA or the target and the location of the RBP relative to the RNA-RNA interaction site can allow inference of the potential lncRNA mechanism.

To solve this problem we propose MechRNA, a pipeline for combining interaction predictions and biological data to discover potential mechanisms. Specifically, this pipeline aims to discover potential mechanisms of an input lncRNA by (1) predicting lncRNA-target interactions using IntaRNA2 with a new feature improving transcriptome-wide performance, (2) identifying RBP binding sites predicted by GraphProt on both the targets and the lncRNA, (3) finding correlation between the lncRNA and targets using TCGA expression or user-provided data, (4) combining this evidence to generate candidate mechanisms, and finally (5) computing joint p-values to select the candidate mechanisms that best explain the observed data.

## 2 Methods

MechRNA has four inputs (Ensembl IDs of lncRNA sequence, target sequences and RBPs, and a list of mechanisms) and two modes (screening and hypothesis-driven modes). In screening mode, the user only specifies the lncRNA, and the entire transcriptome with all available RBP models is used to predict all possible mechanisms. Since nothing is known about the relationships between the lncRNA, targets and RBPs, correlation data is used to reduce the number of candidates. Hypothesis-driven mode allows the user to specify any *a priori* information they may have on the lncRNA. For example, a common case would be that the lncRNA was experimentally shown to downregulate a set of targets. In this case, the user would specify a list of all downregulatory mechanisms from those that are available, and the list of suspected targets. From these inputs, MechRNA predicts lncRNA-target interactions, RBP binding sites and determines the most likely mechanism given these interactions. Here we will describe each stage in detail. An overview of the pipeline is shown in Figure 1.

### 2.1 Sequence Decomposition by Accessibility

Since IntaRNA2 uses accessibility to predict RNA-RNA interactions, areas of low accessibility can be removed from the search space. An

added benefit of this approach is that long transcripts can be naturally split into smaller sequences that can be analyzed independently. Since IntaRNA2 complexity increases quadratically with sequence length, sequence splitting makes cases tractable that are intractable otherwise, i.e., even transcripts with length >20kb can be considered. To accomplish a proper splitting, we developed a new algorithm that incrementally detects the least accessible (most structured) positions in the sequence to be used as split positions. The minimal number of splits are selected that are necessary to make every subsequence shorter than a user-specified length and for each of these subsequences to contain no position less accessible than its split positions. A default maximum length threshold of 1500 nt was selected to ensure that the memory usage does not exceed the typical amount of RAM on a PC or the per-core resource availability of a computing cluster. It should be noted that the majority of transcripts are less than the default threshold and therefore the heuristic will usually not be used, i.e., it is mainly applicable to extreme cases.

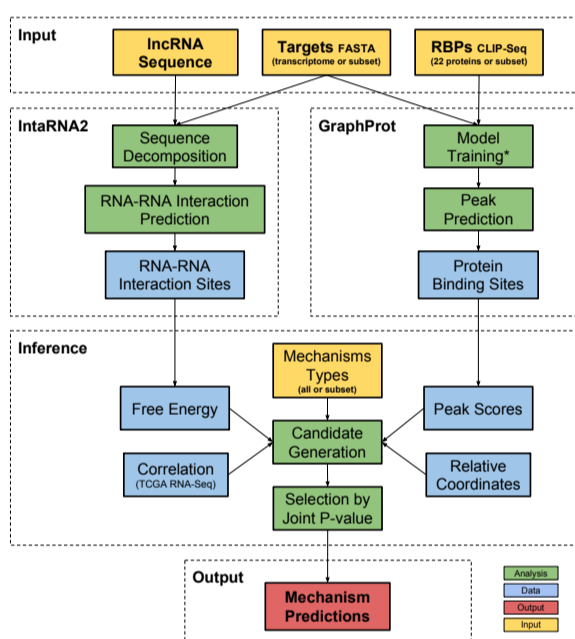


**Fig. 1.** Overview of the MechRNA pipeline. IntaRNA2 computes the optimal RNA-RNA interaction sites between the lncRNA and the accessible regions of targets/transcriptome. GraphProt predicts protein binding sites for all specified RBPs on all targets and the lncRNA. Information derived from these predictions, as well as correlation data, is used to generate candidate mechanisms. Finally, the candidate with the lowest joint p-value is selected for each lncRNA-target pair, and a output list of mechanisms is produced. (\*) Since at the time of publication only 22 RBP CLIP-Seq datasets were available for non-splicing related, post-transcriptional regulation proteins.

The algorithm finds the minimal set of most structured points at which to split a long input sequence according to a given length restriction as follows: Given a sequence  $S$ , the algorithm begins with position  $x = 0$  and  $y = |S| - l$  where  $l$  is a fixed window length (IntaRNA seed length by default). First, the algorithm computes  $\max_i(ED(i, i + l))$ , where  $x \leq i \leq y$  and  $ED$  is the accessibility energy for that range. Accessibility energy is the energy required for a region of RNA to be single stranded, inversely proportional to the probability of the bases being paired in that region, and computed via the partition function. With the detected position  $i$ , a new interval  $(i+l, |S|-1)$  is created and put on the stack. Furthermore, for the current interval,  $y$  is updated to  $i - 1$ . This process is repeated until  $y - x + 1$  is less than the length threshold, at which time it is added to the final list of intervals. The algorithm then moves to the next interval from the stack, i.e., the interval created in the last iteration. The iteration continues

until the last interval is reached (the first interval created with endpoint  $|S| - l$ ). Highly structured regions will produce many maximum  $ED$  windows in close proximity, so a minimum interval length is enforced (again, IntaRNA seed length by default) and regions shorter than this minimum are discarded. The final output is a set of intervals, which are then used as input for IntaRNA. More specifically, IntaRNA will sequentially go through each interval and find the optimal hybridization of the lncRNA with the subsequence contained within the interval. An example execution is shown in Figure 2.

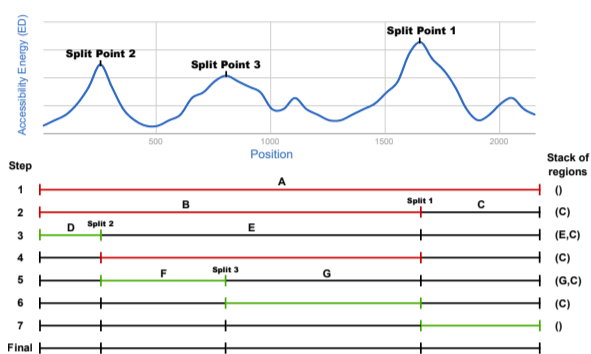


**Fig. 2.** Example execution of the splitting algorithm with a max sequence length of 1000 nt, where the red interval is the one being processed. (1) The first iteration starts with the entire sequence which is longer than the threshold. (2) The first split occurs at the position with max ED at ~ 1700 nt. (3) The interval is still too long, so a second split is made at the next position of max ED at ~ 250 nt. (4) The interval is now below the threshold so the iteration continues to the next interval. (5) This interval is over the threshold and is split at ~ 800 nt. (6-7) The next two intervals are below the threshold. (final) The end result is four intervals, all below the length threshold and more accessible than their split positions.

In a test with 100 random sequences of length over 1500 nt, the algorithm reduced the runtime by 13% and peak memory usage by 65%. Since peak memory has a constant upper bound when using this approach, the peak usage reduction is even more dramatic for extreme cases. It must be noted that the full accessibility matrix for the entire target/lncRNA structure is used for computing hybridization energies, and is reused for each interval within a target. This allows us to limit the search space of possible hybrids as described without any loss in optimality. In other words, any interaction calculated in an accessible region using subsequences of the input RNAs will be identical to those computed using the full input sequences. In the test above, out of the top 10% of predictions using the vanilla algorithm, 95% of them were identical to those found when using the decomposition. This number increases to 97% when we allow for small differences in predicted sites. The only case where an “optimal” interaction may be missed is if a highly energetic hybrid exists between highly structured regions of both RNAs where the difference in energy is still greater than the difference in energy for interactions in more accessible regions. It is unclear whether this type of interaction actually occurs in nature as such interactions exhibit slow kinetics.

## 2.2 RNA-RNA Interaction Predictions

The next stage is the prediction of RNA-RNA interactions using IntaRNA2 (Mann *et al.*, 2017) with the modifications outlined above. Details on the IntaRNA2 algorithm can be found in Supplementary Section 1. IntaRNA2 is executed with the parameters `-tAccL 150 -tAccW 200 -qAccL 150 -qAccW 200 -n 5 -tRegionLenMax 1500`. The `AccL` and `AccW` options used by RNAplfold within IntaRNA2 are recommended by Lange *et al.* (Lange *et al.*, 2012). The `n` option specifies the number of predictions (optimal + suboptimal). The

`tRegionLenMax` option specifies the maximum length of an accessible sequence. This value was selected based on the available computational resources and the average RNA length in the reference transcriptomes. This reduces the usage of the heuristic to minimize the effect on the sensitivity of the algorithm.

MechRNA can run IntaRNA2 on a standard machine or distribute the computation across multiple jobs on a computing cluster. Interactions are predicted between the lncRNA and one of the two reference transcriptomes (Ensembl GRCh37.75 and GRCh38.86). The transcriptomes include all mRNA and ncRNA transcripts, excluding sequences less than 40 nt. This threshold was selected in order to include primary miRNA transcripts while removing dubious, unclassified transcripts. A subset of these transcriptomes is used if the user specifies a list of targets. Once all predictions are completed, the top most energetic interactions (default 3%) are selected for further analysis. P-values are computed for each of these interactions using a distribution estimated from the free energies of all interactions (details in Supplementary Section 2.1).

### 2.3 RNA-Protein Interaction Predictions

For determining RBP binding sites on transcripts, we rely on publicly available CLIP-Seq data. However, since CLIP-Seq depends on transcript expression, binding sites on transcripts specific to certain cell types or conditions cannot be recovered. As we want to study interactions across a reference transcriptome including lncRNAs specifically expressed in certain cancers, we would consequently miss many sites by relying only on direct binding evidence from CLIP-Seq. Therefore, to comprehensively capture protein binding information into our interaction models, we used GraphProt to create transcriptome-wide binding site predictions for 22 RBPs which are known to participate in post-transcriptional gene regulation and influence transcript stability. As an example, using this approach we successfully predicted the interaction between hnRNP-L and the lncRNA DSCAM-AS1, for which there were no reads present in the hnRNP-L CLIP-Seq data (Niknafs *et al.*, 2016). Based on the binding sites inferred from CLIP-Seq data for a given RBP, GraphProt learns its binding preferences and integrates these into a predictive model, incorporating either sequence (referred to as sequence model) or sequence and structure information combined (referred to as structure model). A detailed description of the algorithm can be found in Maticzka *et al.* (Maticzka *et al.*, 2014).

For the 22 RBPs we trained 20 sequence and 8 structure models based on various CLIP-Seq data sources (Table 1). Models for each RBP were selected based on their performance in 10-fold-cross validation, preferring models with higher ROC (area under the receiver operating characteristic) and APR (mean average precision) values. The trained models were then used to predict nucleotide-wise binding score profiles (GraphProt setting: `-action predict_profile`) on two different reference transcriptomes (described in the previous section). Nucleotide-wise profile scores were further averaged with a sliding window approach, taking all scores up to 5 nt up- and downstream of the score position to calculate the new average score. Peaks were extracted from the average score profiles, where a peak is defined as the maximum score in a contiguous region of positive scores. In order to estimate score significancies and to make scores comparable between models, p-values for each peak score were calculated (details in Supplementary Section 2.2).

### 2.4 Correlation Data from TCGA Prostate Tumor Samples

If screening mode is selected, correlation data is also incorporated for all RNA-RNA and RNA-protein pairs predicted in the previous stages. To obtain correlation data we used the GeneNet R package (Schafer and Strimmer, 2005). This approach first computes partial correlations for every pair of genes. The partial correlation is the correlation when the effects of all other variables (genes) are negated. These partial correlations

Table 1. List of RBPs used in the analysis including the source CLIP-Seq data and model type.

Gene ID	Gene Symbol	Protein	Model Type	Protocol	Reference
ENSG00000092199	HNRNPC	hnRNP C	Sequence	eCLIP	(Van Nostrand <i>et al.</i> , 2016)
ENSG00000165119	HNRNPK	hnRNP K	Sequence	eCLIP	(Van Nostrand <i>et al.</i> , 2016)
ENSG00000066044	ELAVL1	HuR	Sequence	PAR-CLIP	(Mukherjee <i>et al.</i> , 2011)
ENSG00000102081	FMR1	FMR-1	Structure	eCLIP	(Van Nostrand <i>et al.</i> , 2016)
ENSG00000121774	KHDRBS1	Sam68	Structure	eCLIP	(Van Nostrand <i>et al.</i> , 2016)
ENSG00000172660	TAF15	TAF15	Sequence	PAR-CLIP	(Hoell <i>et al.</i> , 2011)
ENSG00000092847	AGO1	argonaute	Structure	PAR-CLIP	(Hafner <i>et al.</i> , 2010)
ENSG00000123908	AGO2	argonaute-2	Structure	PAR-CLIP	(Hafner <i>et al.</i> , 2010)
ENSG00000126070	AGO3	argonaute-3	Structure	PAR-CLIP	(Hafner <i>et al.</i> , 2010)
ENSG00000134698	AGO4	argonaute-4	Structure	PAR-CLIP	(Hafner <i>et al.</i> , 2010)
ENSG00000182944	EWSR1	EWS	Structure	eCLIP	(Van Nostrand <i>et al.</i> , 2016)
ENSG00000089280	FUS	FUS	Sequence	PAR-CLIP	(Hoell <i>et al.</i> , 2011)
ENSG00000159217	IGF2BP1	IGF2BP1	Structure	PAR-CLIP	(Hafner <i>et al.</i> , 2010)
ENSG00000073792	IGF2BP2	IGF2BP2	Structure	PAR-CLIP	(Hafner <i>et al.</i> , 2010)
ENSG00000136231	IGF2BP3	IGF2BP3	Structure	PAR-CLIP	(Hafner <i>et al.</i> , 2010)
ENSG00000155363	MOV10	MOV-10	Sequence	PAR-CLIP	(Sievers <i>et al.</i> , 2012)
ENSG00000055917	PUM2	Pumilio-2	Sequence	eCLIP	(Van Nostrand <i>et al.</i> , 2016)
ENSG00000112531	QKI	Hqk	Structure	eCLIP	(Van Nostrand <i>et al.</i> , 2016)
ENSG00000120948	TARDBP	TDP-43	Sequence	eCLIP	(Van Nostrand <i>et al.</i> , 2016)
ENSG00000116001	TIA1	TIA-1	Sequence	eCLIP	(Van Nostrand <i>et al.</i> , 2016)
ENSG00000090905	TNRC6A	TNRC6A	Structure	eCLIP	(Van Nostrand <i>et al.</i> , 2016)
ENSG00000197157	SND1	SND1	Structure	eCLIP	(Van Nostrand <i>et al.</i> , 2016)

are then used to create a graph where each edge is assigned a p-value. We used default parameters and a FDR cutoff of 0.2 to obtain the final correlation network. We deliberately allow a false discovery rate of 20% since the main information will be provided by the RNA-RNA and RNA-protein interactions.

The gene expression data used for correlation computation was derived from The Cancer Genome Atlas (TCGA) (Weinstein *et al.*, 2013) patient samples. Specifically, this includes 551 RNA-Seq samples, 499 tumor and 52 normal. Only the tumor samples were used in the analysis. The raw read counts were normalized using DeSeq2 (Love *et al.*, 2014). All genes with an average read count less than 1 were removed, resulting in 32,709 genes (coding/non-coding).

### 2.5 Combining Evidence

At this stage we incorporate the RNA-RNA and RNA-protein predictions in order to infer a potential mechanism for the lncRNA. For each target transcript, all combinations of RNA-RNA and RNA-protein interactions are classified into candidate mechanisms as shown in Figure 3. The number of combinations is reduced by considering the *a priori* information provided by the user and known functions of the RBPs (for example, HuR is primarily known to stabilize its bound RNA (Srikantan and Gorospe, 2012)). In screening mode, the correlations are also used at this stage to determine if a candidate mechanism is valid. For example, let a target RNA have a peak for RBP *A* and *B*, a lncRNA has a peak for *C*, and the RNA-RNA interaction between the two overlaps at the *A* peak. *A* is positively correlated with the target, *B*, *C*, and the lncRNA are negatively correlated with the target. Then the following tuples would be generated, where  $([target\_peak], [lncRNA\_peak], [mechanism\_type])$  and a dash indicates absence of binding:

- $(-, -, direct\_downregulation)$
- $(A, -, competitive\_downregulation)$
- $(-, C, localization\_downregulation)$
- $(B, -, destabilization)$
- $(A, C, competitive\_downregulation)$
- $(B, C, complex\_downregulation)$

An explanation of each mechanism type with known examples is shown in Table 2. Decoy and direct RBP mechanisms are not included

Table 2. Descriptions of known lncRNA mechanisms. Mechanisms in italics are not included in the predictions.

Mechanism	Description	Example
<i>Direct RBP</i>	RBP interaction directly impacts the target or lncRNA	hnRNPL binding to DSCAM-AS1 (Niknafs <i>et al.</i> , 2016)
<i>Direct RNA</i>	RNA-RNA interaction directly impacts the target with no RBP involvement	TINCR stabilization of various mRNAs (Kretz <i>et al.</i> , 2013)
<i>(De-)Stabilization</i>	RNA-RNA interaction increases/decreases the affinity of RBP binding nearby	iNOS stabilization by AS via HuR (Matsui <i>et al.</i> , 2008)
<i>Localization</i>	RBP bound to the lncRNA is brought into the vicinity of the target through RNA-RNA interaction	MALAT1 localization of splicing factors (Bernard <i>et al.</i> , 2010)
<i>Decoy</i>	RBP is sequestered from the target by the lncRNA	Gas5-AS binding transcription factors (Kino <i>et al.</i> , 2010)
<i>Competitive</i>	RBP and lncRNA compete for the same binding location on the target	7SL disrupts HuR stabilization of TP53 (Abdelmohsen <i>et al.</i> , 2014)
<i>dsRNA Binding</i>	A dsRNA binding protein interacts with stems created from lncRNA interaction	STAU1-mediated decay (Kim <i>et al.</i> , 2007)
<i>Complex</i>	The lncRNA facilitates the formation of a complex between multiple proteins	HOTAIR and the polycomb complex (Zhang <i>et al.</i> , 2014)

in the predictions since they do not include RNA-RNA interactions, making target prediction too non-specific (fully dependant on correlations). Double-stranded RNA binding mechanisms are not predicted either since the CLIP-Seq protocol does not capture such interactions.

The free energies of the RNA-RNA interactions and the peak scores of the RNA-protein interactions both have associated p-values. As mentioned before, each lncRNA-target and protein-target pair of correlations also has a p-value. These p-values can be used to quantitatively assess whether one mechanism is more likely than another. This requires the combining of up to six p-values (depending on the number of interactions involved) into a single p-value for each candidate. The intuitive way to accomplish this is to multiply the p-values together, however this is not correct since the product of p-values is not uniform under the null model. To solve this problem, we use the Stouffer's Z-score method (Stouffer, 1949), which involves computing the sum of the inverse of a normal distribution of each p-value, followed by normalization. This approach also allows for weighting p-values, but we set all weights to be equal. The final output of the pipeline is the list of potential mechanisms sorted and filtered by the joint p-values.

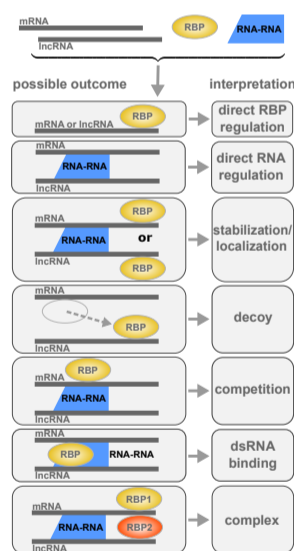


Fig. 3. Illustration of the possible mechanisms that can be inferred from RNA-RNA and RNA-protein interactions.

### 3 Results and Discussion

We selected 8 lncRNAs to analyze using MechRNA, as summarized in Table 3. 7SL (Abdelmohsen *et al.*, 2014), PCAT1 (Prensner *et al.*, 2011) and ARlnc1 (Accepted in principle, Zhang *et al.* Nature Genetics 2018) recently investigated lncRNAs with known roles in prostate cancer and mechanistic hypotheses, are used to test the hypothesis-driven mode. The remaining 5 lncRNA are used to test the screening mode.

PCA3 (Bussemakers *et al.*, 1999) and PCAT29 (Malik *et al.*, 2014) are well-studied prostate cancer related lncRNAs without a known mechanism. SSTR5-AS1 is one of the highest expressed lncRNAs in neuroendocrine prostate cancer (NEPC) and LINC00514 is one of the highest persistently expressed lncRNAs identified in the neuroendocrine transdifferentiation (NEtD) process, which is shown to cause NEPC (Ramnarine *et al.*, unpublished). Finally we selected TINCR (Kretz *et al.*, 2013) as a well known regulator of cell differentiation mediated by interaction with target mRNAs.

Table 3. Selected lncRNAs for MechRNA analysis. The lncRNAs vary in terms of what is known about their mechanisms, allowing MechRNA to be tested with various amounts of a priori data. PCAT1 has a question mark indicating that competitive binding is the hypothesis not been validated yet.

lncRNA	Length	Target	Protein Binding	Mechanism	Cancer Type
7SL	299	TP53	HuR	Competitive	Prostate
PCAT1	1992	BRCA2	HuR	Competitive?	Prostate
ARlnc1	2786	AR	Unknown	Unknown	Prostate
PCA3	3922	Unknown	Unknown	Unknown	Prostate
PCAT29	694	Unknown	Unknown	Unknown	Prostate
LINC00514	3385	CLDN9	Unknown	Unknown	NEPC
SSTR5-AS1	2864	SSTR5	Unknown	Unknown	NEPC
TINCR	3733	STAU1	Many	Stabilization	Various

#### 3.1 Hypothesis-driven Mode Results on Prostate Cancer lncRNAs

We first tested our hypothesis-driven mode with three prostate cancer lncRNAs. The first lncRNA is 7SL, which we use as a validation case since it has a good deal of evidence supporting the proposed mechanism. The next two lncRNAs, PCAT1 and ARlnc1, are less understood and so we aim to build a more complete picture of their potential mechanisms.

##### 3.1.1 7SL Downregulation of TP53 through Competitive Binding with HuR (ELAVL1)

Abdelmohsen *et al.* (Abdelmohsen *et al.*, 2014) provided the first experimental evidence supporting a competitive lncRNA mechanism. 7SL is a housekeeping ncRNA which is part of the signal recognition particle (SRP) ribonucleoprotein complex, but also leads to increased cell proliferation when over-expressed in cancer cells. It was demonstrated that 7SL binds to the transcript of the tumor suppressor TP53 near HuR binding sites, preventing HuR from binding and subsequently reducing the stability of TP53. The experimentally validated RNA-RNA interaction was between nucleotide positions 10-56, 256-298 of 7SL and positions 2167-2300 of TP53 (ENST00000269305). Using PAR-CLIP data they determined that HuR binds at positions 2125-2160, 2452-2472 and 2531-2556.

For this case we ran MechRNA with 16 protein-coding TP53 transcripts as targets, all downregulatory mechanisms and all RBP models. For all 16

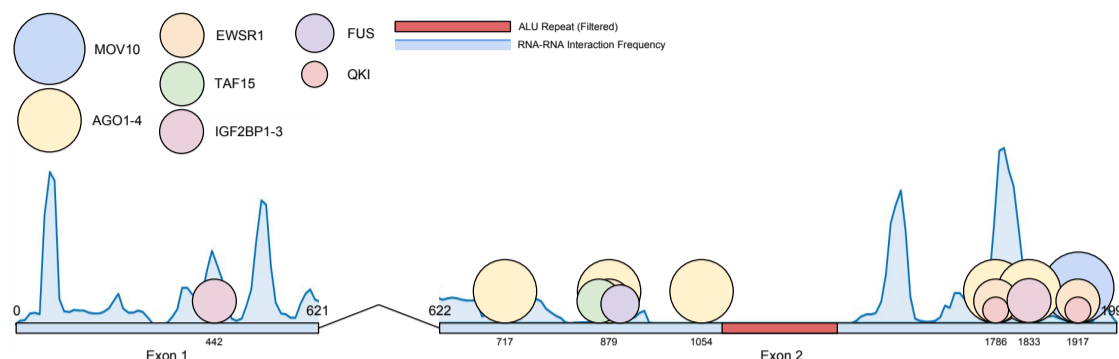


**Fig. 4.** Distribution of RNA-RNA and RNA-protein interactions for PCAT1. The circles represent proteins and have a diameter relative to their molecular masses. The blue regions are a histogram of the frequency of RNA-RNA binding of each position with other transcripts.

transcripts, “competitive downregulation” with HuR was predicted to be the most likely mechanism ( $p < 10^{-15}$  for the combined p-value as described in section 2.5). The predicted binding locations of 7SL and HuR for each transcript are shown in Supplementary Table 2. The IntaRNA2 interaction prediction was in agreement with the crude BLAST search done in the experimental study. The 10-56 (actually 10-96 is more energetically favorable) interaction was also predicted but not included in the final results since it is not close enough to the HuR binding site to have an effect. In terms of RBP binding, GraphProt only predicts the 2125-2160 as significant when compared to all HuR binding across the transcriptome. This demonstrates the superiority of using GraphProt over raw PAR-CLIP data. We also show here that this mechanism appears to be ubiquitous across splice variants of TP53.

Another RBP, EWS, was included in this prediction. GraphProt detected a binding site for EWS on 7SL at 140-161, in between the two RNA-RNA interaction sites. EWS is best known for its role in Ewing sarcoma through its translocation with other genes. However, wildtype EWS also acts as a translation repressor by causing mRNA to be retained in the nucleus (Huang *et al.*, 2014). It may be that EWS is aiding in the displacement of HuR and furthering the downregulation of TP53.

### 3.1.2 PCAT1 Downregulation of BRCA2 through Competitive Binding with HuR (ELAVL1)

PCAT1 was identified by Prensner *et al.* (Prensner *et al.*, 2011) as the most differentially expressed lncRNA in prostate cancer. Shortly afterwards it was discovered that this lncRNA regulates the important tumor suppressor BRCA2 (Prensner *et al.*, 2014). Specifically, it was shown that PCAT1 reduces BRCA2 mRNA stability and that the first 250 nt of PCAT1 were essential for this process. Furthermore, they demonstrated that this regulation was occurring via the BRCA2 3'UTR. Since mRNA stability was decreased, our hypothesis is that a similar mechanism to 7SL exists for PCAT1 and BRCA2, so we used the same parameters of all downregulatory mechanisms and all RBP models. For this analysis we used the BRCA2 3'UTR from the RefSeq transcript as it was used in Prensner *et al.* (Prensner *et al.*, 2011).

Figure 4 summarizes the interaction predictions by showing the frequency of interaction for each position of PCAT1 and the significant RBP binding peaks. Our findings appear to support that the first 250 nt play an important role due to high frequency of interaction with targets and no significant binding with RBPs. The predicted mechanism was “competitive downregulation” (combined p-value  $p < 10^{-4}$ ) involving HuR on the 3'UTR. The RNA-RNA interaction is between 11204-11237 on BRCA2 and 65-90 on PCAT1 (-12.493 kcal/mol), with a HuR peak at 11216-11236 on BRCA2. There are also two other HuR binding sites predicted

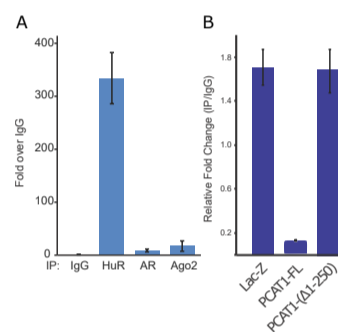


**Fig. 5.** (A) IgG/HuR/AR/Ago2 proteins were immunoprecipitated by antibodies in LNCaP cells and the bound BRCA2 RNA was detected by qPCR. The result confirms binding of BRCA2 mRNA to HuR protein in cells. (B) RWPE cells stably expressing lac-Z, PCAT1-FL or PCAT1-delta-1-250 were harvested. HuR was immunoprecipitated using anti-HuR antibody and bound RNA (BRCA2) was detected by qPCR. As shown in A, HuR can bind to BRCA2. In presence of FL-PCAT1 this binding is inhibited. In presence of PCAT1-delta-1-250 there was no effect on HuR and BRCA2 binding. The result confirms the role of PCAT1 in mediating BRCA2-HuR binding.

by GraphProt downstream and upstream of the interaction site with similar binding affinity.

To validate this mechanism experimentally, we first confirmed that HuR indeed binds to BRCA2 3'UTR. As shown in Figure 5A, immunoprecipitation of HuR in LNCaP cells pulled down more BRCA2 mRNA than the IgG control. Next, we conducted a competitive binding assay in RWPE cells. This assay immunoprecipitated HuR using an anti-HuR antibody and the bound RNA (BRCA2) was detected by qPCR. In the presence of unmodified PCAT1 the amount of bound BRCA2 RNA was reduced. When using a modified PCAT1 construct with the first 250 nt deleted, there was no effect on the amount of bound BRCA2. This suggests that an interaction involving the 5' end of PCAT1 is competitively reducing the amount of HuR bound to BRCA2 (Figure 5B).

### 3.1.3 ARlnc1 Upregulatory Feedback Loop with Androgen Receptor

ARlnc1 has recently been identified as an upregulator of Androgen Receptor (AR) in prostate cancer (Accepted in principle, Zhang *et al.* Nature Genetics 2017). In turn, AR upregulates ARlnc1, leading to a positive feedback loop contributing to cancer progression. The mechanism was identified with the aid of the first stage of MechRNA, which predicted an RNA-RNA interaction between ARlnc1 and the 3'UTR of AR. However, how exactly ARlnc1 upregulates AR remains unclear. Similarly to 7SL, we ran MechRNA with all RBPs on all AR protein coding transcripts, but with all upregulation mechanisms.

The most common and important AR transcript, ENST00000374690, as well as two other splice variants (ENST00000612452, ENST00000396044) had predicted mechanisms involving the experimentally validated interaction at 815-851 on ARlnc1 (-35.8 kcal/mol). In all three cases, a “stabilization” mechanism was predicted (respectively  $p < 10^{-6}$ ,  $p < 10^{-5}$ ,  $p < 10^{-4}$  for the combined p-values) involving the protein Sam68, which has a strong binding site upstream of the ARlnc1 interaction on the AR 3'UTR. In agreement, Sam68 3'UTR interaction has been shown to enhance target translation (Paronetto *et al.*, 2009). Sam68 is known to increase AR-V7 (ENST00000504326) expression (Stockley *et al.*, 2015), but the authors observed that upregulation of AR-V7 (and full-length) was still present when using a mutated exonic splicing enhancer (ESE) site. They suggested a synergistic stabilization mechanism via the 3'UTR. Although the 3'UTR of AR-V7 and full-length AR is not shared, a similar binding pattern is observed for Sam68 and ARlnc1 in the AR-V7 3'UTR. Our findings appear to support the additional stabilization mechanism they observed and that all major AR isoforms are regulated in the same manner.

### 3.2 Screening Mode Results on Prostate Cancer lncRNAs

We ran MechRNA on all eight lncRNAs (three from the hypothesis-driven analysis and five additional cancer-related lncRNA as described in Table 3) using the entire transcriptome for potential targets for a broad, unbiased screen. This yielded several hundred to several thousand potential targets for each lncRNA. The number of predictions increased with the length of the lncRNA, since longer lncRNAs are more likely to have RNA-RNA and RNA-protein interactions and consequently more viable combinations of interactions, indicating potential mechanisms. Since our focus here is on cancer, we extracted predicted mechanisms involving known cancer genes from the TSGene (Zhao *et al.*, 2015) and OGene (Liu *et al.*, 2017) database. These mechanisms are shown in Table 4.

As shown in the table, these prostate cancer lncRNAs generally act as positive regulators of oncogenes with the exception of the PCA3-ABI1 and PCAT1-LEFTY2 interaction. Also the most favorable RNA-RNA interactions commonly occur in the 5' and 3' UTRs, as would be expected for post-transcriptional regulation. It is unclear whether the CDS interactions have any functionality. TINCR-DAXX falls within a small simple repeat region which may indicate non-specific binding. Another observation is that PCAT1 and PCA3 share the target gene HOXC13, and even bind to the same location on the HOXC13 transcript. HOXC13 is commonly dysregulated in prostate cancer (Komisarof *et al.*, 2017). It may be that the same phenotype is induced by both lncRNAs.

Our most significant result is an interaction involving AKT1, an important and well-studied prostate cancer gene (Cariaga-Martinez *et al.*, 2013). LINC00514 binds very strongly to the 5'UTR and has a strong positive correlation, implying a direct upregulatory effect. No significant protein binding was detected in the region for the included proteins. This would suggest the lncRNA alone is able to regulate AKT1. We observed several other cases like this, labelled as “direct” in the table. It may be the case that some other RBP, which was not included in our analysis due to missing CLIP data, also interacts with AKT1 in this region. As the number of RBPs with available CLIP data is ever increasing, it is likely that a future run of MechRNA with more RBPs might provide additional evidence.

Another significant result was the predicted competitive downregulation of LEFTY2 by PCAT1. This is the most significant result for PCAT1 involving a known cancer gene. It has a close similarity to the PCAT1-BRCA2 mechanism, as it involves the same part of PCAT1 (61-97) binding to a 3'UTR overlapping a protein binding site (in this case IGF2BP2). LEFTY2 is an important tumor suppressor in endometrial cancer (Alowayed *et al.*, 2016). We do not have data for PCAT1 expression in endometrial cancer, but there is high expression in ovarian and breast cancer (Iyer *et al.*, 2015).

The PCA3-ABI1 mechanism is an interesting example demonstrating the importance of sequence accessibility for interaction prediction. ABI1 is known to negatively regulate cell growth and transformation and is down-regulated in a variety of cancers (Zhang *et al.*, 2015; Chen *et al.*, 2010; Cui *et al.*, 2010). The gene has 11 annotated protein-coding isoforms in Ensembl, 9 of which have an identical 5'UTR sequence. However, 3 of the splice variants exclude exon 3, leading to a much more energetic binding to PCA3 (-13 kcal/mol difference). This is because the exclusion affects the accessibility of the 5'UTR by reducing the probability that this region is bound by intramolecular interactions. If PCA3 is indeed down-regulating ABI1, as the correlation indicates, there may be selection for these isoforms in cancer cells to increase the effect of PCA3. Naive approaches to RNA-RNA interaction prediction computing only the hybridization would not capture the difference in interaction energy between the different splice variants. This is because the sequence of the best hybridization site is always the same, the only feature considered when computing the optimal interaction. However, the accessibility can differ between different isoforms, which may affect the location of the true optimal interaction site, as we see in the case of PCA3-ABI1.

## 4 Conclusion

Recent discoveries of lncRNA mechanisms indicate that there exists a complex interplay between RNA-binding proteins, lncRNAs and their target RNAs. Until now, RNA-RNA and RNA-protein interaction predictions were carried out independently, failing to capture this complexity. Here we present MechRNA, the first tool to integrate both kinds of interactions in order to more accurately predict lncRNA mechanisms. We accomplish this by combining the output of IntaRNA2 and GraphProt into a novel inference tool which determines the most likely combination of interactions. These sets of interactions are then classified into mechanisms using correlation data from publicly available patient gene expression samples or user-defined *a priori* data. We demonstrated the functionality of MechRNA by analyzing 8 prostate cancer lncRNAs with varying amounts of information available with respect to their mechanisms. The results confirm one known mechanism, provide new insights into poorly understood mechanisms and offer new hypotheses for the remaining lncRNAs without known mechanisms. Despite the challenges involved in this kind of analysis (discussed in Supplementary Section 3), our results show that MechRNA is a useful tool for identifying potential roles of lncRNAs in cancer, and for furthering our understanding on lncRNA mechanisms in general.

## Funding

This work has been supported in part by the Indiana University Grand Challenges Program, The Precision Health Initiative and the NSERC Discovery Frontiers Program, The Cancer Genome Collaboratory to SCS. Furthermore, this work has been supported by the Baden-Württemberg-Stiftung (BWST NCRNA 008), the German Research Foundation (DFG grant BA2168/11-1 SPP 1738) and the BMBF Verbundprojekt Deutsches Netzwerk für Bioinformatik-Infrastruktur(de.NBI).

Table 4. Select lncRNA mechanisms predictions for known cancer genes, selected based on rank (joint p-value) and agreement with known roles of the cancer genes and RBPs. Genes in red indicate oncogenes, green indicate tumor suppressors and yellow are uncategorized. The first section indicates the target and how many isoforms (Iso) it interacts with. The next three sections describe the interactions involved. For RNA-RNA, the free energy in kcal/mol (FE) and genomic context are included. For RBP-RNA, the protein name is provided. In all three cases the correlation (+ positive, - negative) and the correlation FDR are shown if applicable. The final section displays the mechanism categorization and the combined p-value.

lncRNA	Target	RNA-RNA Interaction					RBP-Target Interaction			RBP-lncRNA Interaction			Mechanism		
		Gene Symbol	Iso.	FE	Context	Cor.	Cor. FDR	RBP	Cor.	Cor. FDR	RBP	Cor.	Cor. FDR	Type	P-Value
LINC00514	AKT1	3	-65.97	5'UTR	+		$1.3 \times 10^{13}$	none	NA	NA	none	NA	NA	direct	$2.6 \times 10^{20}$
PCAT1	LEFTY2	2	-31.63	3'UTR	-		0.001	IGF2BP2	+	$1.3 \times 10^{13}$	none	NA	NA	competitive	$1.2 \times 10^{19}$
PCAT29	BMPRI1A	1	-28.32	3'UTR	+		0.182	IGF2BP3	+	$2.3 \times 10^{10}$	none	NA	NA	stabilization	$6.6 \times 10^{16}$
PCA3	ABI1	5	-44.55	5'UTR	-		0.023	TAF15	+	0.111	none	NA	NA	de-stabilization	$6.8 \times 10^{15}$
PCAT1	HOXC13	1	-26.57	5'UTR	+		$1.3 \times 10^{13}$	none	NA	NA	none	NA	NA	direct	$4.8 \times 10^{14}$
LINC00514	FLI1	1	-60.4096	5'UTR	+		0.083	EWSR1	-	0.006	none	NA	NA	competitive	$5.5 \times 10^{14}$
SSTR5-AS1	TP53	7	-33.18	3'UTR	+		0.006	HNRNPC	+	0.081	none	NA	NA	stabilization	$1.6 \times 10^{13}$
SSTR5-AS1	RAC1	1	-32.97	3'UTR	+		0.159	KHDRBS1	+	$4.1 \times 10^{05}$	none	NA	NA	stabilization	$2.2 \times 10^{13}$
SSTR5-AS1	HLF	5	-27.25	3'UTR	+		$2.4 \times 10^{07}$	none	NA	NA	none	NA	NA	direct	$5.6 \times 10^{13}$
PCA3	HOXC13	1	-48.02	5'UTR	+		0.013	none	NA	NA	none	NA	NA	direct	$1.7 \times 10^{12}$
ARln1	CAMK1D	1	-27.7706	5'UTR	+		$1.4 \times 10^{11}$	none	NA	NA	none	NA	NA	direct	$2.0 \times 10^{12}$
TINCR	DAXX	7	-106.10	CDS	none		NA	none	NA	NA	IGF2BP2	+	0.046	localization	$2.7 \times 10^{12}$
PCAT1	CCND1	1	-30.86	3'UTR	+		0.007	ELAVL1	+	0.001	none	NA	NA	stabilization	$1.1 \times 10^{11}$
ARln1	BRD4	2	-31.95	3'UTR	+		0.039	ELAVL1	+	0.052	none	NA	NA	stabilization	$3.0 \times 10^{11}$
LINC00514	CHD4	4	-36.99	CDS	+		0.029	TAF15	+	0.002	none	NA	NA	stabilization	$7.2 \times 10^{11}$
PCAT29	ALK	2	-32.85	CDS	+		$4.6 \times 10^{07}$	none	NA	NA	none	NA	NA	direct	$8.6 \times 10^{11}$
TINCR	NAB2	3	-66.93	5'UTR	none		NA	none	NA	NA	IGF2BP2	+	0.045	localization	$5.4 \times 10^{09}$

## References

- Abdelmohsen, K., et al. (2014). 7SL RNA represses p53 translation by competing with HuR. *Nucleic Acids Res.*, **42**(15), 10099–10111.
- Alkan, C., et al. (2006). RNA-RNA interaction prediction and antisense RNA target search. *J. Comput. Biol.*, **13**(2), 267–282.
- Alkan, F., et al. (2017). Rlsearch2: suffix array-based large-scale prediction of RNA-RNA interactions and siRNA off-targets. *Nucleic Acids Res.*, **45**(8), e60.
- Alowayed, N., et al. (2016). LEFTY2 Controls Migration of Human Endometrial Cancer Cells via Focal Adhesion Kinase Activity (FAK) and miRNA-200a. *Cell. Physiol. Biochem.*, **39**(3), 815–826.
- Andronescu, M., Zhang, Z. C., and Condon, A. (2005). Secondary structure prediction of interacting RNA molecules. *J. Mol. Biol.*, **345**(5), 987–1001.
- Bailey, T. L. and Elkan, C. (1994). Fitting a mixture model by expectation maximization to discover motifs in biopolymers. *Proc Int Conf Intell Syst Mol Biol*, **2**, 28–36.
- Bernard, D., et al. (2010). A long nuclear-retained non-coding RNA regulates synaptogenesis by modulating gene expression. *EMBO J.*, **29**(18), 3082–3093.
- Bernhart, S. H., et al. (2006). Partition function and base pairing probabilities of RNA heterodimers. *Algorithms Mol Biol*, **1**(1), 3.
- Brunner, A. L., et al. (2012). Transcriptional profiling of long non-coding rnas and novel transcribed regions across a diverse panel of archived human cancers. *Genome biology*, **13**(8), R75.
- Bussemakers, M. J., et al. (1999). DD3: a new prostate-specific gene, highly overexpressed in prostate cancer. *Cancer Res.*, **59**(23), 5975–5979.
- Cariaga-Martinez, A. E., et al. (2013). Distinct and specific roles of AKT1 and AKT2 in androgen-sensitive and androgen-independent prostate cancer cells. *Cell. Signal.*, **25**(7), 1586–1597.
- Chen, H., et al. (2010). Integrity of SOS1/EPS8/ABI1 tri-complex determines ovarian cancer metastasis. *Cancer Res.*, **70**(23), 9979–9990.
- Chitsaz, H., et al. (2009). A partition function algorithm for interacting nucleic acid strands. *Bioinformatics*, **25**(12), i365–373.
- Cui, M., et al. (2010). Downregulation of ABI1 expression affects the progression and prognosis of human gastric carcinoma. *Med. Oncol.*, **27**(3), 632–639.
- Djebali, S., et al. (2012). Landscape of transcription in human cells. *Nature*, **489**(7414), 101–108.
- Hafner, M., et al. (2010). Transcriptome-wide identification of RNA-binding protein and microRNA target sites by PAR-CLIP. *Cell*, **141**(1), 129–141.
- Hiller, M., et al. (2006). Using RNA secondary structures to guide sequence motif finding towards single-stranded regions. *Nucleic Acids Res.*, **34**(17), e117.
- Hoell, J. I., et al. (2011). RNA targets of wild-type and mutant FET family proteins. *Nat. Struct. Mol. Biol.*, **18**(12), 1428–1431.
- Huang, F. W., et al. (2009). Partition function and base pairing probabilities for RNA-RNA interaction prediction. *Bioinformatics*, **25**(20), 2646–2654.
- Huang, L., Kuwahara, I., and Matsumoto, K. (2014). EWS represses coflin 1 expression by inducing nuclear retention of coflin 1 mRNA. *Oncogene*, **33**(23), 2995–3003.
- Iyer, M. K., et al. (2015). The landscape of long noncoding RNAs in the human transcriptome. *Nat. Genet.*, **47**(3), 199–208.
- Kato, Y., et al. (2010). RactIP: fast and accurate prediction of RNA-RNA interaction using integer programming. *Bioinformatics*, **26**(18), i460–466.
- Kazan, H., et al. (2010). RNAcontext: a new method for learning the sequence and structure binding preferences of RNA-binding proteins. *PLoS Comput. Biol.*, **6**, e1000832.
- Kim, Y. K., et al. (2007). Staufen1 regulates diverse classes of mammalian transcripts. *EMBO J.*, **26**(11), 2670–2681.
- Kino, T., et al. (2010). Noncoding RNA gas5 is a growth arrest- and starvation-associated repressor of the glucocorticoid receptor. *Sci Signal*, **3**(107), ra8.
- Kiryu, H., et al. (2011). A detailed investigation of accessibilities around target sites of siRNAs and miRNAs. *Bioinformatics*, **27**(13), 1788–1797.
- Komisarof, J., et al. (2017). A four gene signature predictive of recurrent prostate cancer. *Oncotarget*, **8**(2), 3430–3440.
- Konig, J., et al. (2010). iCLIP reveals the function of hnRNP particles in splicing at individual nucleotide resolution. *Nat. Struct. Mol. Biol.*, **17**(7), 909–915.
- Kretz, M., et al. (2013). Control of somatic tissue differentiation by the long non-coding RNA TINCR. *Nature*, **493**(7431), 231–235.
- Kung, J. T., Colognori, D., and Lee, J. T. (2013). Long noncoding RNAs: past, present, and future. *Genetics*, **193**(3), 651–669.
- Lange, S. J., et al. (2012). Global or local? Predicting secondary structure and accessibility in mRNAs. *Nucleic Acids Res.*, **40**(12), 5215–5226.
- Liu, S. J., et al. (2016). Single-cell analysis of long non-coding rnas in the developing human neocortex. *Genome biology*, **17**(1), 67.
- Liu, Y., Sun, J., and Zhao, M. (2017). Ongene: A literature-based database for human oncogenes. *Journal of Genetics and Genomics*, **16**, 1–620.
- Lorenz, R., et al. (2011). ViennaRNA Package 2.0. *Algorithms Mol Biol*, **6**, 26.
- Love, M. I., Huber, W., and Anders, S. (2014). Moderated estimation of fold change and dispersion for RNA-seq data with DESeq2. *Genome Biol.*, **15**(12), 550.
- Malik, R., et al. (2014). The lncRNA PCAT29 inhibits oncogenic phenotypes in prostate cancer. *Mol. Cancer Res.*, **12**(8), 1081–1087.
- Mann, M., Wright, P. R., and Backofen, R. (2017). IntaRNA 2.0: enhanced and customizable prediction of RNA-RNA interactions. *Nucleic Acids Res.*
- Marchese, F. P., Raimondi, I., and Huarte, M. (2017). The multidimensional mechanisms of long noncoding rna function. *Genome biology*, **18**(1), 206.
- Maticzka, D., et al. (2014). GraphProt: modeling binding preferences of RNA-binding proteins. *Genome Biol.*, **15**(1), R17.
- Matsui, K., et al. (2008). Natural antisense transcript stabilizes inducible nitric oxide synthase messenger RNA in rat hepatocytes. *Hepatology*, **47**(2), 686–697.
- Muckstein, U., et al. (2006). Thermodynamics of RNA-RNA binding. *Bioinformatics*, **22**(10), 1177–1182.
- Mukherjee, N., et al. (2011). Integrative regulatory mapping indicates that the rna-binding protein hur couples pre-mrna processing and mrna stability. *Molecular cell*, **43**(3), 327–339.
- Niknafs, Y. S., et al. (2016). The lncrna landscape of breast cancer reveals a role for dscam-as1 in breast cancer progression. *Nature communications*, **7**, 12791.

- Paronetto, M. P., *et al.* (2009). Sam68 regulates translation of target mRNAs in male germ cells, necessary for mouse spermatogenesis. *The Journal of cell biology*, **185**(2), 235–249.
- Prensner, J. R., *et al.* (2011). Transcriptome sequencing across a prostate cancer cohort identifies PCAT-1, an unannotated lincRNA implicated in disease progression. *Nat. Biotechnol.*, **29**(8), 742–749.
- Prensner, J. R., *et al.* (2014). PCAT-1, a long noncoding RNA, regulates BRCA2 and controls homologous recombination in cancer. *Cancer Res.*, **74**(6), 1651–1660.
- Rehmsmeier, M., *et al.* (2004). Fast and effective prediction of microRNA/target duplexes. *RNA*, **10**(10), 1507–1517.
- Salari, R., Backofen, R., and Sahinalp, S. C. (2010). Fast prediction of RNA-RNA interaction. *Algorithms Mol Biol*, **5**, 5.
- Schafer, J. and Strimmer, K. (2005). An empirical Bayes approach to inferring large-scale gene association networks. *Bioinformatics*, **21**(6), 754–764.
- Sievers, C., *et al.* (2012). Mixture models and wavelet transforms reveal high confidence RNA-protein interaction sites in MOV10 par-clip data. *Nucleic acids research*, **40**(20), e160–e160.
- Srikantan, S. and Gorospe, M. (2012). HuR function in disease. *Front Biosci (Landmark Ed)*, **17**, 189–205.
- Stockley, J., *et al.* (2015). The RNA-binding protein Sam68 regulates expression and transcription function of the androgen receptor splice variant AR-V7. *Sci Rep*, **5**, 13426.
- Stouffer, S. (1949). *The American soldier. Vol. 1: Adjustment during army life. Studies in social psychology in World War II.* Princeton University Press.
- Terai, G., *et al.* (2016). Comprehensive prediction of lncRNA-RNA interactions in human transcriptome. *BMC Genomics*, **17** Suppl 1, 12.
- Uhl, M., *et al.* (2017). Computational analysis of clip-seq data. *Methods*.
- Van Nostrand, E. L., *et al.* (2016). Robust transcriptome-wide discovery of RNA binding protein binding sites with enhanced clip (eclip). *Nature methods*, **13**(6), 508.
- Weinstein, J. N., *et al.* (2013). The Cancer Genome Atlas Pan-Cancer analysis project. *Nat. Genet.*, **45**(10), 1113–1120.
- Wright, P. R., *et al.* (2013). Comparative genomics boosts target prediction for bacterial small RNAs. *Proc. Natl. Acad. Sci. U.S.A.*, **110**(37), E3487–3496.
- Wright, P. R., *et al.* (2014). CopraRNA and IntaRNA: predicting small RNA targets, networks and interaction domains. *Nucleic Acids Res.*, **42**(Web Server issue), W119–123.
- Zarnegar, B. J., *et al.* (2016). irclip platform for efficient characterization of protein-RNA interactions. *Nature methods*, **13**(6), 489.
- Zhang, J., *et al.* (2014). Long non-coding RNA HOTAIR in carcinogenesis and metastasis. *Acta Biochim. Biophys. Sin. (Shanghai)*, **46**(1), 1–5.
- Zhang, J., *et al.* (2015). Upregulation of Abelson interactor protein 1 predicts tumor progression and poor outcome in epithelial ovarian cancer. *Hum. Pathol.*, **46**(9), 1331–1340.
- Zhao, M., *et al.* (2015). Tsgene 2.0: an updated literature-based knowledgebase for tumor suppressor genes. *Nucleic acids research*, **44**(D1), D1023–D1031.